Tight-binding simulation of current-carrying nanostructures

You may also be interested in:

Power dissipation in nanoscale conductors
M J Montgomery, T N Todorov and A P Sutton

Non-linear conductance of disordered quantumwires
T N Todorov

Atomistic theory of transport
Alessandro Pecchia and Aldo Di Carlo

Inelastic current–voltage spectroscopy of atomic wires
M J Montgomery, J Hoekstra, T N Todorov et al.

Electron–phonon interaction in atomic-scale conductors
M J Montgomery and T N Todorov

Elastic quantum transport through small structures
T N Todorov, G A D Briggs and A P Sutton

Quantum transport through mesoscopic disordered interfaces, junctions, andmultilayers
Branislav K Nikoli

B-splines in atomic and molecular physics
H Bachau, E Cormier, P Decleva et al.

Dynamical simulation of inelastic quantum transport
Eunan J McEniry, D R Bowler, Daniel Dundas et al.

Tight-binding simulation of current-carrying nanostructures

Tchavdar N Todorov

School of Mathematics and Physics, Queen's University of Belfast, Belfast BT7 1NN, UK

Abstract
The tight-binding (TB) approach to the modelling of electrical conduction in
small structures is introduced. Different equivalent forms of the TB expression
for the electrical current in a nanoscale junction are derived. The use of the
formalism to calculate the current density and local potential is illustrated
by model examples. A first-principles time-dependent TB formalism for
calculating current-induced forces and the dynamical response of atoms is
presented. An earlier expression for current-induced forces under steady-state
conditions is generalized beyond local charge neutrality and beyond orthogonal
TB. Future directions in the modelling of power dissipation and local heating
in nanoscale conductors are discussed.

1. Introduction

The study of the mechanical, chemical and transport properties of nanoscale structures is a
dynamic modern subject, defining an interface between physics, chemistry, materials science,
engineering and biology. Structures accessible to experimental and theoretical study in this field
range from atomic-scale metallic contacts, atomic chains, clusters and molecules to structures,
such as carbon nanotubes and DNA molecules, with lengths of many thousands of atoms. In a
typical transport experiment, a given nanostructure of interest is placed between two electrodes
and a bias is applied between the electrodes, resulting in the flow of electrical current through
the nanostructure. Such experiments pose two fundamental theoretical questions. The first
is: how do the differential conductance and the current–voltage characteristics of the circuit
depend on the positions and chemical identity of the atoms in the nanostructure, and on the
nature of the electrodes and their coupling to the nanostructure? The second is: what is the
effect of conduction on the mechanical properties of the nanostructure, and, in particular, how
does current flow affect interatomic forces and the temperature in the nanostructure?

These questions require an approach that allows one to describe simultaneously, at the
atomistic level, the quantum mechanical motion of electrons and the interaction between
electrons and individual nuclei in the conducting system. The free-electron model, TB and
density functional theory (DFT) have all been applied to the nanoscale transport problem.

As is often the case in electronic structure theory, this progression of models represents varying degrees of compromise between numerical and conceptual tractability on the one hand and quantitative accuracy on the other. The choice of method in any particular problem depends on the purpose of the investigation and on the taste of the researcher. The particular strengths of TB that the author has encountered in his own work are the following. First, it is the simplest model that allows one to take explicit account of atomistic structure, and to track the relation between atomistic structure and conduction properties. Second, TB allows mechanical structure, transport and current-induced mechanical effects to be treated within a transparent common conceptual framework, namely on the basis of the concept of the interatomic bond. Third, since TB involves the expansion of electron wavefunctions in a discrete positional basis, namely an atomic orbital basis, many mathematical results of the TB transport formalism are directly transferable to any other electronic model, if that model is to be solved on a discrete computational mesh [1–4]. Fourth, the relatively modest size of TB basis sets pays off in the size of systems that are open to TB transport simulations.

The strengths of the TB approach to transport are illustrated by the range of problems to which it has been applied. TB has been used to model the operation of the scanning tunnelling microscope (STM), with and without adsorbates, over a range of tip–substrate separations [5–17]. TB is employed to calculate the differential conductance and current–voltage characteristics of molecular wires [18–35]. It can be used to study the transport properties of long disordered quantum wires in the ballistic, diffusive and localization regimes [36–46]. TB has been applied to the modelling of transport in, and STM imaging of, carbon nanotubes [40, 47–72]. TB has been successful in the study of transport in metal–insulator–metal tunnel junctions, spin valves and magnetic multilayers [73–88]. The TB transport formalism, combined with molecular dynamics simulations, was used to relate the experimentally measured conductance of an atomic-scale metallic contact to the evolution of the underlying atomistic geometry and structure of the contact during contact formation and fracture [89–91]. TB has been used to relate the conduction properties of atomic-scale metallic contacts and atomic chains to the detailed chemistry of the metal atoms [92–98]. Recently, a TB formalism was developed to calculate changes to interatomic bonding forces under electrical current flow in atomic-scale conductors [99, 100]. This formalism allows intrinsic forces, the electrical current and current-induced forces to be calculated simultaneously, within a single, internally consistent calculation. The method is sufficiently efficient to enable structural relaxation and atomic movements to be performed in the simulation, which in turn makes it possible to calculate current-induced changes to activation barriers and rates for various atomic rearrangements. The formalism has been used to model electromigration and current-induced fracture of atomic wires [101, 102].

An exhaustive review of the literature in any one of the above areas would constitute a daunting task. The aim of the present article is to give an introduction to the physical and mathematical principles of the TB approach to transport in a unified way that would be of use to researchers in any one of these areas. First, we will consider the TB description of electrical current flow. Various commonly used forms of the TB result for the total current, and differential conductance, in a nanojunction are derived, and the equivalence between them is demonstrated. The calculation of the local current density and local potential in the presence of current flow is illustrated by model numerical examples. We then consider the TB simulation of current-induced mechanical effects. A general time-dependent (TD) TB formalism for calculating forces on atoms in the presence of transport, and the dynamical response of atoms to these forces, is presented [103]. Under steady-state conditions, in the limit of local charge neutrality (LCN), an earlier result for current-induced forces is recovered. This result is generalized beyond charge neutrality and beyond orthogonal TB models. Future directions in

the simulation of power dissipation and local heating in nanojunctions are outlined. A one-electron picture is used throughout. Electron–electron interactions and self-consistency are treated in a mean-field picture.

2. Tight-binding transport formalism: set-up and fundamental quantities

2.1. Representation of the circuit

The fundamental set-up considered in this paper is shown in figure 1 [36, 38, 104]. The conducting system consists of two semi-infinite electrodes, to be referred to as lead 1 and lead 2, connected by an intermediate region, to be referred to as the sample. In fact, the division of the system into these regions is nominal, because, as is explained below, the assumptions that we make about the leads and the sample are general and unrestrictive. No constraint is imposed on the dimensionality, transverse size and transverse shape of the leads. They can be one-dimensional atomic chains, two-dimensional planar atomic strips or three-dimensional wires of arbitrary cross-section. The sample is a cluster of atoms of arbitrary size, structure, geometry and composition. Thus, the sample could be a single atom or an atomic chain, connecting the leads. It could be a molecule, or a metallic connective neck, representing a nanoscale constriction. The lead–sample–lead assembly could represent an STM junction, with or without an adsorbate. The sample may be an insulating barrier. The sample and leads may all have the same uniform cross-section, in which case the lead–sample–lead system constitutes a single continuous piece of wire of uniform thickness. We, furthermore, may always redefine the leads and sample by including parts of each lead into the region that we are calling the sample, or vice versa. The only definite assumption that we make about the structure of the system is that far away from the sample region each lead is a perfect defect-free crystalline conductor with a uniform cross-section.

We will, for now, ignore atomic motion and assume that at any instant in time the electrons in the system see a frozen, static set of atomic positions. In other words, for now we allow only elastic electron scattering. The justification for this approximation is that in many cases the inelastic electron mean free path is much larger than the typical dimension of the sample region, and, therefore, as far as the motion of the electrons in that region is concerned, we may to a good approximation ignore electron–phonon scattering. Extensions of the transport formalism beyond the elastic regime are given for example in references [105, 106]. Here, we will return to the question of electron–phonon interactions later, in connection with local heating at high current densities.

Next, we imagine that at infinity each lead is connected through a smooth contact to a macroscopic conductor, acting as a particle reservoir. The electrochemical potential [107] of reservoir 1, μ_1, is raised relative to that of reservoir 2, μ_2, by an amount eW, $\mu_1 = \mu_2 + eW$. Positive eW corresponds to electron flow from left to right. Each reservoir injects electrons into its respective lead with the Fermi–Dirac distribution function appropriate to that reservoir, resulting in a net steady-state flow of current through the lead–sample–lead system. One way of achieving the bias is to connect a battery of battery voltage W across the reservoirs, as indicated in figure 1. Another way would be to deposit appropriate macroscopic charges on the reservoirs, in which case the system becomes a capacitor, discharging quasistatically through the lead–sample–lead system. In a calculation, to model for example a metallic nanocontact between macroscopic electrodes, one might take the leads to have an infinite transverse size compared with the sample [89–91, 99, 102]. In that case the distinction between leads and reservoirs disappears, and the leads themselves may be thought of as reservoirs [108, 109].
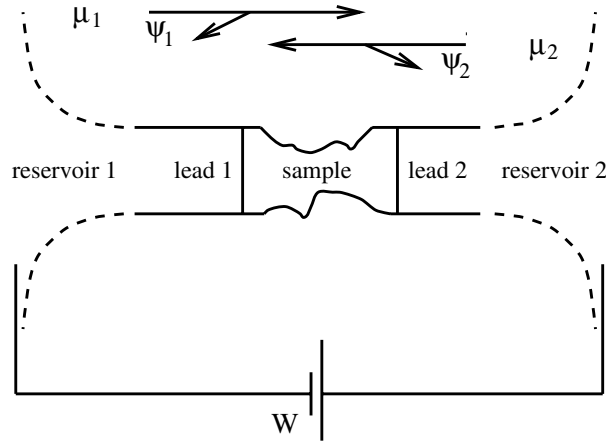
Figure 1. The general conducting system considered in the paper. The intermediate sample region can have an arbitrary atomistic geometry and composition. Far away from the sample each semi-infinite lead is a defect-free crystalline conductor of uniform cross-section. At infinity, each lead is connected through a smooth contact to a particle reservoir, acting as a battery terminal. The details are discussed in the text.

2.2. Electronic structure of the circuit

A one-electron picture is employed throughout this paper. The one-electron eigenstates of the lead–sample–lead system, whether calculated self-consistently or not, and whether calculated within a free-electron jellium model [110], TB [36] or DFT [111], may be divided into two groups [36, 99, 104]. One group, $\{|\psi_1\rangle\}$ with energies $\{E_1\}$, which will be referred to as right-travelling states, consist of a right-travelling incident electron wave in lead 1, scattered in the sample region, partially reflected back into lead 1 and partially transmitted into lead 2. The other group, $\{|\psi_2\rangle\}$ with energies $\{E_2\}$, which will be referred to as left-travelling states, consist of a left-travelling incident electron wave in lead 2, scattered in the sample region, partially reflected back into lead 2 and partially transmitted into lead 1. Reservoir 1 populates the right-travelling states with a population function $f_1(E)$ and reservoir 2 populates the left-travelling states with a population function $f_2(E) = f_1(E + eW)$, where $f_1(E)$ and $f_2(E)$ are the Fermi–Dirac distribution functions for the two respective reservoirs [36, 99, 104]. Then the electrons in the current-carrying lead–sample–lead system are described by the Hermitian one-electron density operator

$$\Omega(W) = \int f_1(E) D_1(E) \, \mathrm{d}E + \int f_2(E) D_2(E) \, \mathrm{d}E \tag{1}$$

where

$$D_1(E) = \sum_1 |\psi_1\rangle \delta(E - E_1) \langle\psi_1| \tag{2}$$

$$D_2(E) = \sum_2 |\psi_2\rangle \delta(E - E_2) \langle\psi_2| \tag{3}$$

are the partial density-of-states operators associated with the right- and left-travelling states respectively. $D_1(E)$ and $D_2(E)$ are related by

$$D_1(E) + D_2(E) = D(E) \tag{4}$$

where $D(E)$ is the full density of states operator for the lead–sample–lead system. In a self-consistent calculation, the states $\{|\psi_1\rangle\}$ and $\{|\psi_2\rangle\}$ are themselves functions of the applied bias W [99, 111].

For simplicity, here we have assumed that the lead–sample–lead system does not have bound states. In fact, bound states are common. For example, an infinite regular atomic chain, containing a single atom that is different from the rest, will in general have one or more bound states, centred at that atom. Although we will not consider bound states explicitly here, such states can in general be accommodated in the formalism both when they lie outside the energy continuum of conducting states and in the special case of bound states embedded in the continuum.

2.3. Tight-binding representation of the electron states

The defining feature of TB is the expansion of one-electron states in a localized atomic orbital basis $\{|\phi_{n\gamma}\rangle\}$, where $|\phi_{n\gamma}\rangle$ is an atomic orbital of type γ, centred at atomic site n. In this basis, a general electron state $|\psi\rangle$ is written as

$$|\psi\rangle = \sum_{n,\gamma} \psi_{n\gamma} |\phi_{n\gamma}\rangle \tag{5}$$

where $\{\psi_{n\gamma}\}$ are expansion coefficients. We will not consider spin-polarized systems and will assume that the basis states $\{|\phi_{n\gamma}\rangle\}$, and the states $\{|\psi_1\rangle\}$ and $\{|\psi_2\rangle\}$, do not carry a spin label. Spin degeneracy is thus to be introduced via the distribution functions $f_1(E)$ and $f_2(E)$ in equation (1).

In this paper, as far as the description of current flow, discussed in sections 2–5, is concerned, we will ignore the overlap of different positional basis states. This stipulation may be expressed as

$$\langle \phi_{n\gamma} | \phi_{n'\gamma'} \rangle = \delta_{nn'} \delta_{\gamma\gamma'}. \tag{6}$$

In doing so, we may wish to preserve our view of the basis states $\{|\phi_{n\gamma}\rangle\}$ as actual atomic orbitals. Then equation (6) must be viewed as an approximation, whose quality is controlled by the magnitude of the overlap that exists in reality. Alternatively, we may view $|\phi_{n\gamma}\rangle$ as an abstract positional basis with an inner product, defined by equation (6). This is the view taken in solving quantum mechanical transport problems on a discrete computational grid [1–4]. Extensions of the transport formalism to non-orthogonal TB models may be found for instance in [30, 34, 35, 53, 71, 72, 97, 112, 113]. In this paper, we will consider non-orthogonal models later on, in connection with TD TB and current-induced forces.

In the orthogonal positional basis, the Hermitian TB one-electron Hamiltonian is written as

$$\mathcal{H} = \sum_{n,\gamma,n',\gamma'} |\phi_{n\gamma}\rangle \mathcal{H}_{n\gamma n'\gamma'} \langle \phi_{n'\gamma'}|. \tag{7}$$

The TB Hamiltonian matrix elements $\mathcal{H}_{n\gamma n'\gamma'} = \mathcal{H}^*_{n'\gamma'n\gamma}$ will in general depend in a self-consistent manner on the instantaneous electron density in the system [99]. Such self-consistent contributions to $\mathcal{H}_{n\gamma n'\gamma'}$ will be discussed in detail in connection with TD TB and current-induced forces. In a self-consistent calculation, the effective one-particle TB Hamiltonian $\mathcal{H}$ will, furthermore, be a function of the applied bias W [99]. The diagonal TB Hamiltonian matrix elements are often referred to as on-site energies, and the off-diagonal ones as hopping integrals. We will assume here that the hopping integrals have an arbitrary but finite spatial range. Let us also define the general notation $A_{n\gamma n'\gamma'}$ by

$$A = \sum_{n,\gamma,n',\gamma'} |\phi_{n\gamma}\rangle A_{n\gamma n'\gamma'} \langle \phi_{n'\gamma'}| \tag{8}$$

for any TB one-electron operator A, expressed in the orthogonal positional basis $\{|\phi_{n\gamma}\rangle\}$. In this orthogonal basis, A and $A_{n\gamma n'\gamma'}$ are related by $A_{n\gamma n'\gamma'} = \langle \phi_{n\gamma} | A | \phi_{n'\gamma'} \rangle$.

In an orthogonal TB model with frozen atomic positions, a general one-electron state $|\psi(t)\rangle = \sum_{n,\gamma} \psi_{n\gamma}(t)|\phi_{n\gamma}\rangle$ satisfies the TD Schrödinger equation (SE)

$$\mathcal{H}|\psi(t)\rangle = i\hbar|\dot{\psi}(t)\rangle \tag{9}$$

or, in matrix form,

$$\sum_{n',\gamma'} \mathcal{H}_{n\gamma n'\gamma'}\psi_{n'\gamma'}(t) = i\hbar\dot{\psi}_{n\gamma}(t). \tag{10}$$

If $|\psi\rangle$ is an eigenstate of $\mathcal{H}$, then it satisfies the time-independent SE

$$\mathcal{H}|\psi\rangle = E|\psi\rangle \tag{11}$$

or, in matrix form,

$$\sum_{n',\gamma'} \mathcal{H}_{n\gamma n'\gamma'}\psi_{n'\gamma'} = E\psi_{n\gamma} \tag{12}$$

where E is the respective energy eigenvalue.

2.4. Bond current operator and total current operator

Let us define the projection operator

$$P_n = \sum_{\gamma} |\phi_{n\gamma}\rangle\langle\phi_{n\gamma}|. \tag{13}$$

This operator represents the electron occupancy of atomic site n. The $\{P_n\}$ satisfy the closure relation

$$\sum_n P_n = \mathbf{1} \tag{14}$$

where $\mathbf{1}$ is the identity operator within the Hilbert space spanned by the orthogonal positional basis $\{|\phi_{n\gamma}\rangle\}$. Let us now seek the operator, J_n, representing the rate of change of the occupation of site n. Let $|\psi(t)\rangle$ be a general TD electron state, and let $P_n(t) = \langle\psi(t)|P_n|\psi(t)\rangle$. Let us consider the equation of motion of $P_n(t)$ [36, 114, 115]. Equation (9) gives $\dot{P}_n(t) = (1/i\hbar)\langle\psi(t)|[P_n, \mathcal{H}]|\psi(t)\rangle$. We may then identify J_n as [36, 114, 115]

$$\mathsf{J}_n = (1/i\hbar)[P_n, \mathcal{H}] = (1/i\hbar)\sum_{n'\neq n}(P_n\mathcal{H}P_{n'} - P_{n'}\mathcal{H}P_n). \tag{15}$$

From this relation, it is natural to identify the quantity

$$\mathsf{J}_{n'n} = (1/i\hbar)(P_n\mathcal{H}P_{n'} - P_{n'}\mathcal{H}P_n) = (1/i\hbar)\sum_{\gamma,\gamma'}(|\phi_{n\gamma}\rangle\mathcal{H}_{n\gamma n'\gamma'}\langle\phi_{n'\gamma'}| - |\phi_{n'\gamma'}\rangle\mathcal{H}_{n'\gamma' n\gamma}\langle\phi_{n\gamma}|)$$
$$\tag{16}$$

as an operator that represents the electron particle current from site n' into site n [1, 2, 44, 104]. Notionally, this intersite current may be represented by a bundle of flow lines bunched together along the line joining the two sites, and may thus be thought of as a bond current. The bond current operator $\mathsf{J}_{n'n}$ may be obtained also from considerations of the form of the SE on a discrete mesh [1, 2].

The logic of the derivation of the bond current operator above must be revised in the case of non-orthogonal orbitals. In that case, both physically and mathematically, if an electron occupies an orbital on a given atomic site, then, via the non-vanishing overlap, this electron also partially occupies orbitals on neighbouring sites. Therefore, while we may still define the projection operator P_n in equation (13), we may no longer unambiguously interpret the rate of change of the expectation of P_n as the particle current into site n alone. Hence, a possible

strategy in that case might be to use the starting, non-orthogonal orbital basis to construct a new, orthogonal basis, thus reducing the problem to the one considered here. Specific schemes for dealing with the non-orthogonal case are discussed in [30, 34, 35, 53, 71, 72, 97, 112, 113].

Let us now consider the operator, J_S, that represents the total electron particle current across a given open surface S through the system. J_S is given by the sum of bond current operators across S, or [36, 38, 104, 114, 115]

$$J_S = (1/i\hbar) \sum_{n \in R, n' \in L} J_{n'n} \tag{17}$$

$$= (1/i\hbar)(\mathcal{P}_2 \mathcal{H} \mathcal{P}_1 - \mathcal{P}_1 \mathcal{H} \mathcal{P}_2) \tag{18}$$

$$= (1/i\hbar)[\mathcal{P}_2, \mathcal{H}] \tag{19}$$

$$= -(1/i\hbar)[\mathcal{P}_1, \mathcal{H}] \tag{20}$$

where L and R designate the region to the left of S and the region to the right of S, respectively, and

$$\mathcal{P}_1 = \sum_{n \in L} P_n \qquad \mathcal{P}_2 = \sum_{n \in R} P_n \tag{21}$$

$$\mathcal{P}_1 \mathcal{P}_2 = \mathcal{P}_2 \mathcal{P}_1 = 0 \qquad \mathcal{P}_1 \mathcal{P}_1 = \mathcal{P}_1 \qquad \mathcal{P}_2 \mathcal{P}_2 = \mathcal{P}_2 \tag{22}$$

$$\mathcal{P}_1 + \mathcal{P}_2 = \mathbf{1}. \tag{23}$$

As may be seen from equation (18), the operator J_S, when expressed in the positional basis $\{|\phi_{n\gamma}\rangle\}$, contains only a finite number of terms, namely terms that involve atomic sites bonded across S by the TB Hamiltonian.

2.5. The operator D

We will now express the density-of-states operators $D_1(E)$, $D_2(E)$ and $D(E)$ in equations (2)–(4) in terms of the Green operator for the lead–sample–lead system. The susceptibility of the TB method to a formulation in terms of Green functions is a great mathematical and computational strength. We begin with the full density-of-states operator $D(E)$.

The Green operator, $G(z)$, for a Hamiltonian $\mathcal{H}$ with eigenstates $\{|\psi_s\rangle\}$ and eigenenergies $\{E_s\}$ is given by

$$G(z) = \sum_s |\psi_s\rangle (z - E_s)^{-1} \langle\psi_s|. \tag{24}$$

It satisfies

$$(z - \mathcal{H})G(z) = G(z)(z - \mathcal{H}) = \mathbf{1} \tag{25}$$

or, in matrix form,

$$zG_{n\gamma n'\gamma'}(z) - \sum_{n'',\gamma''} G_{n\gamma n''\gamma''}(z)\mathcal{H}_{n''\gamma'' n'\gamma'} = \delta_{nn'}\delta_{\gamma\gamma'} = zG_{n\gamma n'\gamma'}(z) - \sum_{n'',\gamma''} \mathcal{H}_{n\gamma n''\gamma''} G_{n''\gamma'' n'\gamma'}(z) \tag{26}$$

$G(z)$ has the property

$$G(z^*) = G^\dagger(z). \tag{27}$$

Let us also define the retarded and advanced Green operators, $G^\pm(E)$, by

$$G^\pm(E) = \sum_{n,\gamma,n',\gamma'} |\phi_{n\gamma}\rangle G^\pm_{n\gamma n'\gamma'}(E) \langle\phi_{n'\gamma'}| \tag{28}$$

where

$$G^\pm_{n\gamma n'\gamma'}(E) = \lim_{\epsilon \to 0+} G_{n\gamma n'\gamma'}(E \pm i\epsilon) \tag{29}$$
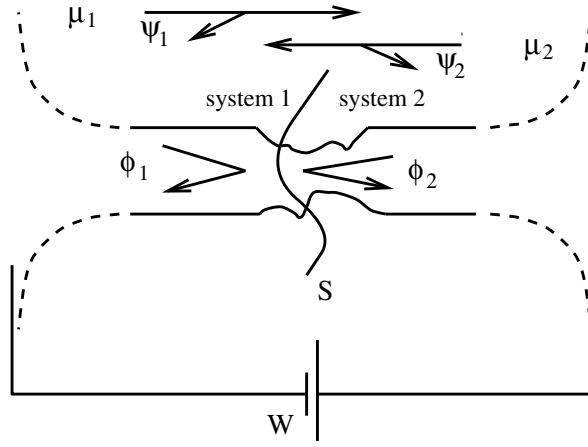
Figure 2. The lead–sample–lead system with one cutting surface, S. The semi-infinite systems 1 and 2, on the left and on the right of S respectively, are described by a TB Hamiltonian obtained from the original Hamiltonian for the lead–sample–lead system by the removal of all hopping integrals intersected by S, possibly accompanied by arbitrary modifications to a finite number of other hopping integrals and on-site energies. The details are discussed in the text.

$G^+(E)$ and $G^-(E)$ have the property

$$G^+(E) = G^{-\dagger}(E). \tag{30}$$

In a self-consistent calculation, like $\mathcal{H}$, the operators $G(z)$ and $G^\pm(E)$ are functions of the bias W [99]. The full density-of-states operator $D(E)$ in equation (4) may now be expressed as

$$2\pi \mathrm{i} D(E) = G^-(E) - G^+(E). \tag{31}$$

2.6. The operators D_1 and D_2 with a cut

In order to express the operators $D_1(E)$ and $D_2(E)$ in equations (1)–(3) in a tractable form, we employ the following trick [104]. Let us choose an arbitrary open surface across the lead–sample–lead system, such as the surface S in figure 2. Let us imagine removing all bonds—which we will assume to be finite in number—intersected by S, so as to separate the lead–sample–lead system into two decoupled systems. In addition to the cut along S, we may, furthermore, make arbitrary modifications to the TB Hamiltonian to the left and to the right of S, so long as these modifications involve only a finite number of atomic sites. This procedure may be summarized by writing

$$\mathcal{H} = \mathcal{H}_0 + \mathcal{V} \tag{32}$$

where

$$\mathcal{V} = \mathcal{P}_1 \mathcal{H} \mathcal{P}_2 + \mathcal{P}_2 \mathcal{H} \mathcal{P}_1 + \mathcal{V}^{(1)} + \mathcal{V}^{(2)}. \tag{33}$$

The first two terms in $\mathcal{V}$ contain the bonds, or hopping integrals, intersected by S, and represent the cut along S. The Hermitian operators $\mathcal{V}^{(1)}$ and $\mathcal{V}^{(2)}$ each have a finite number of non-zero positional matrix elements. $\mathcal{V}^{(1)}_{n\gamma n'\gamma'}$ can be non-zero only if both n and n' lie on the left of S, and $\mathcal{V}^{(2)}_{n\gamma n'\gamma'}$ can be non-zero only if both n and n' lie on the right of S. Within these specifications, $\mathcal{V}^{(1)}$ and $\mathcal{V}^{(2)}$ are arbitrary. The system, described by the Hamiltonian $\mathcal{H}_0 = \mathcal{H} - \mathcal{V}$, consists of two decoupled semi-infinite systems, designated as system 1 and system 2 in figure 2.

Scattering theory tells us that each right-travelling eigenstate of the lead–sample–lead system, $|\psi_1\rangle$ with energy E_1, may be derived from a corresponding eigenstate, $|\phi_1\rangle$, of system 1, with the same energy, via the Lippmann–Schwinger equation [36, 104]

$$|\psi_1\rangle = [1 + G^+(E_1)\mathcal{V}]|\phi_1\rangle. \tag{34}$$

$|\phi_1\rangle$ consists of an incident electron wave in lead 1, scattered back into lead 1 by the severed end. Similarly, each left-travelling eigenstate of the lead–sample–lead system, $|\psi_2\rangle$ with energy E_2, may be derived from a corresponding eigenstate, $|\phi_2\rangle$, of system 2 via

$$|\psi_2\rangle = [1 + G^+(E_2)\mathcal{V}]|\phi_2\rangle. \tag{35}$$

Using equations (34) and (35), we may write equations (2) and (3) as [104]

$$D_1(E) = [1 + G^+(E)\mathcal{V}]d_1(E)[1 + \mathcal{V}G^-(E)] \tag{36}$$
$$D_2(E) = [1 + G^+(E)\mathcal{V}]d_2(E)[1 + \mathcal{V}G^-(E)] \tag{37}$$

where

$$d_1(E) = \sum_1 |\phi_1\rangle\delta(E - E_1)\langle\phi_1| \tag{38}$$

$$d_2(E) = \sum_2 |\phi_2\rangle\delta(E - E_2)\langle\phi_2|. \tag{39}$$

Here, $d_1(E)$ and $d_2(E)$ are the density-of-states operators for the decoupled systems 1 and 2, respectively. They may be expressed in terms of the corresponding Green operators as follows.

Let $g(z)$ be the Green operator, corresponding to the Hamiltonian $\mathcal{H}_0$ in equation (32), with $(z - \mathcal{H}_0)g(z) = g(z)(z - \mathcal{H}_0) = \mathbf{1}$. $G(z)$ and $g(z)$ are related by the Dyson equations

$$G(z) = g(z) + g(z)\mathcal{V}G(z) = g(z) + G(z)\mathcal{V}g(z). \tag{40}$$

Let $g^+(E)$ and $g^-(E) = g^{+\dagger}(E)$ be defined by

$$g^\pm(E) = \sum_{n,\gamma,n',\gamma'} |\phi_{n\gamma}\rangle g^\pm_{n\gamma n'\gamma'}(E)\langle\phi_{n'\gamma'}| \tag{41}$$

where

$$g^\pm_{n\gamma n'\gamma'}(E) = \lim_{\epsilon\to 0+} g_{n\gamma n'\gamma'}(E \pm i\epsilon) \tag{42}$$

$G^\pm(E)$ and $g^\pm(E)$ are related by the Dyson equations

$$G^\pm(E) = g^\pm(E) + g^\pm(E)\mathcal{V}G^\pm(E) = g^\pm(E) + G^\pm(E)\mathcal{V}g^\pm(E). \tag{43}$$

Let

$$g_1^\pm(E) = \mathcal{P}_1 g^\pm(E) = g^\pm(E)\mathcal{P}_1 \tag{44}$$
$$g_2^\pm(E) = \mathcal{P}_2 g^\pm(E) = g^\pm(E)\mathcal{P}_2. \tag{45}$$

$g_1^\pm(E)$ and $g_2^\pm(E)$ are the retarded and advanced Green operators for the two decoupled systems 1 and 2, respectively [36, 104]. Then

$$2\pi i d_1(E) = g_1^-(E) - g_1^+(E) \tag{46}$$
$$2\pi i d_2(E) = g_2^-(E) - g_2^+(E). \tag{47}$$

Equations (36) and (37), together with (46) and (47), constitute a useful form for the partial density-of-states operators $D_1(E)$ and $D_2(E)$.

2.7. The operators D_1 and D_2 without a cut

Equations (36) and (37) involve the Green operators for the two decoupled systems 1 and 2 in figure 2. However, our original definition of the right- and left-travelling states, $\{|\psi_1\rangle\}$ and $\{|\psi_2\rangle\}$, did not involve, or refer to, any particular choice of cutting surface S, or any of the other ingredients of $\mathcal{V}$ in equation (33). Therefore, it must be possible to express $D_1(E)$ and $D_2(E)$ in a form which involves solely the properties of the original lead–sample–lead system. This may be done as follows [104].

Using equations (43) and (44), we may cast equation (36) as

$$2\pi i D_1(E) = \mathcal{P}_1 G^-(E) - G^+(E)\mathcal{P}_1 + G^+(E)(\mathcal{V}\mathcal{P}_1 - \mathcal{P}_1\mathcal{V})G^-(E)$$
$$= \mathcal{P}_1 G^-(E) - G^+(E)\mathcal{P}_1 + G^+(E)(\mathcal{P}_2\mathcal{V}\mathcal{P}_1 - \mathcal{P}_1\mathcal{V}\mathcal{P}_2)G^-(E) \quad (48)$$

where, for the second line, we have used equation (23). Since $\mathcal{H}_0$ contains no hopping integrals between systems 1 and 2, we may write $\mathcal{P}_2\mathcal{H}_0\mathcal{P}_1 = \mathcal{P}_1\mathcal{H}_0\mathcal{P}_2 = 0$, and hence $\mathcal{P}_2\mathcal{V}\mathcal{P}_1 - \mathcal{P}_1\mathcal{V}\mathcal{P}_2 = \mathcal{P}_2\mathcal{H}\mathcal{P}_1 - \mathcal{P}_1\mathcal{H}\mathcal{P}_2$. Therefore, following a similar procedure for $D_2(E)$, we may cast equations (36) and (37) as [104]

$$2\pi i D_1(E) = \mathcal{P}_1 G^-(E) - G^+(E)\mathcal{P}_1 + G^+(E)(\mathcal{P}_2\mathcal{H}\mathcal{P}_1 - \mathcal{P}_1\mathcal{H}\mathcal{P}_2)G^-(E) \quad (49)$$

$$2\pi i D_2(E) = \mathcal{P}_2 G^-(E) - G^+(E)\mathcal{P}_2 + G^+(E)(\mathcal{P}_1\mathcal{H}\mathcal{P}_2 - \mathcal{P}_2\mathcal{H}\mathcal{P}_1)G^-(E). \quad (50)$$

Equations (49) and (50) contain only quantities defined for the original lead–sample–lead system. These equations no longer contain any reference to the cut described by $\mathcal{V}$. That cut was merely a device to obtain these equations. As in the case of the current operator J_S in equation (18), the expressions inside the brackets in equations (49) and (50), when expressed in the positional basis, contain only a finite number of terms, namely terms that involve atomic sites bonded across S by the TB Hamiltonian.

Equations (49) and (50) still contain the projection operators $\mathcal{P}_1$ and $\mathcal{P}_2$, which were defined with respect to a particular surface S. However, since $D_1(E)$ and $D_1(E)$ were originally defined without reference to any such surface, the right-hand sides of equations (49) and (50) must in fact be independent of the surface used to define $\mathcal{P}_1$ and $\mathcal{P}_2$ [104]. To see this, let us first define

$$2\pi i D_1(E, \epsilon) = \mathcal{P}_1 G(z^*) - G(z)\mathcal{P}_1 + G(z)(\mathcal{P}_2\mathcal{H}\mathcal{P}_1 - \mathcal{P}_1\mathcal{H}\mathcal{P}_2)G(z^*) \quad (51)$$

where $z = E + i\epsilon$, with ϵ a small positive real number. For any finite ϵ, the matrix elements of $G(z)$ and $G(z^*)$ in the positional basis $\{|\phi_{n\gamma}\rangle\}$ decay exponentially with distance along the semi-infinite leads. If $[D_1(E)]_{n\gamma n'\gamma'}$ and $[D_1(E, \epsilon)]_{n\gamma n'\gamma'}$ are matrix elements of $D_1(E)$ and $D_1(E, \epsilon)$, respectively, in the positional basis, then

$$[D_1(E)]_{n\gamma n'\gamma'} = \lim_{\epsilon \to 0^+} [D_1(E, \epsilon)]_{n\gamma n'\gamma'}. \quad (52)$$

Let us now choose some other open surface S', and let $\mathcal{P}_1'$ and $\mathcal{P}_2'$ be the analogues of $\mathcal{P}_1$ and $\mathcal{P}_2$, defined with respect to S'. Let $D_1'(E)$ be given by equation (49) with $\mathcal{P}_1$ and $\mathcal{P}_2$ replaced by $\mathcal{P}_1'$ and $\mathcal{P}_2'$, respectively. Let $D_1'(E, \epsilon)$ be given by equation (51) with $\mathcal{P}_1$ and $\mathcal{P}_2$ replaced by $\mathcal{P}_1'$ and $\mathcal{P}_2'$, respectively. As in equation (52),

$$[D_1'(E)]_{n\gamma n'\gamma'} = \lim_{\epsilon \to 0^+} [D_1'(E, \epsilon)]_{n\gamma n'\gamma'}. \quad (53)$$

Let us now invoke equation (23) in order to replace $\mathcal{P}_2\mathcal{H}\mathcal{P}_1 - \mathcal{P}_1\mathcal{H}\mathcal{P}_2$ in the right-hand side of equation (51) by $\mathcal{H}\mathcal{P}_1 - \mathcal{P}_1\mathcal{H}$. Then, from equations (25) and (27),

$$2\pi i D_1(E, \epsilon) = G(z)\mathcal{P}_1 G(z^*)(z - z^*) \quad (54)$$

and similarly

$$2\pi i D_1'(E, \epsilon) = G(z)\mathcal{P}_1' G(z^*)(z - z^*) \quad (55)$$

Although $\mathcal{P}_1$ and $\mathcal{P}'_1$ involve summations over infinitely many sites along lead 1, the exponential decrease of the positional matrix elements of $G(z)$ and $G(z^*)$ with distance along the lead ensures that the right-hand sides of equations (54) and (55) are well defined.

Equations (54) and (55) give

$$2\pi\mathrm{i}[D'_1(E, \epsilon) - D_1(E, \epsilon)] = G(z)\,\Delta\mathcal{P}\,G(z^*)(z - z^*) \tag{56}$$

where $\Delta\mathcal{P} = \mathcal{P}'_1 - \mathcal{P}_1$. The projection operator $\Delta\mathcal{P}$ contains only a finite number of atomic sites, namely those enclosed between S and S'. Hence, for any given n, γ, n' and γ', in the limit $\epsilon \to 0^+$ the quantity $\{[D'_1(E, \epsilon)]_{n\gamma n'\gamma'} - [D_1(E, \epsilon)]_{n\gamma n'\gamma'}\}$ tends to zero as $(z - z^*) = 2\mathrm{i}\epsilon$. Hence, recalling equations (52) and (53), $[D'_1(E)]_{n\gamma n'\gamma'}] = [D_1(E)]_{n\gamma n'\gamma'}$. Therefore, the positional matrix elements of $D_1(E)$, and hence also those of $D_2(E) = D(E) - D_1(E)$, are independent of the choice of open surface S, used to define $\mathcal{P}_1$ and $\mathcal{P}_2$ in equation (49). Hence, in a calculation that employs the positional basis, the operators $D_1(E)$ and $D_2(E)$ may be treated as independent of S [104]. The choice of surface in equations (49) and (50) is a matter of convenience.

3. Zero-current theorem

Given the TB density operator $\Omega(W)$ in equation (1), the expectation value of any TB operator A is given by

$$\mathrm{Tr}[A\Omega(W)] = \sum_{n,\gamma,n',\gamma'} A_{n\gamma n'\gamma'}[\Omega(W)]_{n'\gamma'n\gamma}. \tag{57}$$

Thus, the average electron particle bond current, $J_{n'n}$, from site n' into site n, and the average total current, J_S, crossing a surface S, are given by

$$J_{n'n} = \mathrm{Tr}[\mathrm{J}_{n'n}\Omega(W)] \tag{58}$$

$$J_S = \mathrm{Tr}[\mathrm{J}_S\Omega(W)] \tag{59}$$

where $\mathrm{J}_{n'n}$ and J_S are the bond current operator and the total current operator, introduced earlier.

We now assume that we may always find a set of on-site unitary transformations $\{U^{(n)}\}$ with

$$|\tilde{\phi}_{n\gamma}\rangle = \sum_{\gamma'} U^{(n)}_{\gamma\gamma'}|\phi_{n\gamma'}\rangle \qquad U^{(n)*}_{\gamma\gamma'} = U^{(n)-1}_{\gamma'\gamma} \tag{60}$$

such that $\mathcal{H}$, and hence also $G(z)$, $G^{\pm}(E)$ and $D(E)$, is a symmetric matrix in the transformed positional basis $\{|\tilde{\phi}_{n\gamma}\rangle\}$. This assumption is plausible in the absence of magnetic fields. Then

$$\mathrm{Tr}[\mathrm{J}_{n'n}D(E)] = (1/\mathrm{i}\hbar)\sum_{\gamma,\gamma'}\{\mathcal{H}_{n\gamma n'\gamma'}[D(E)]_{n'\gamma'n\gamma} - [D(E)]_{n\gamma n'\gamma'}\mathcal{H}_{n'\gamma'n\gamma}\}$$

$$= (1/\mathrm{i}\hbar)\sum_{\gamma,\gamma'}\{\tilde{\mathcal{H}}_{n\gamma n'\gamma'}[\tilde{D}(E)]_{n'\gamma'n\gamma} - [\tilde{D}(E)]_{n\gamma n'\gamma'}\tilde{\mathcal{H}}_{n'\gamma'n\gamma}\} = 0 \tag{61}$$

where $\tilde{\mathcal{H}}_{n\gamma n'\gamma'} = \langle\tilde{\phi}_{n\gamma}|\mathcal{H}|\tilde{\phi}_{n'\gamma'}\rangle = \tilde{\mathcal{H}}_{n'\gamma'n\gamma}$, $[\tilde{D}(E)]_{n\gamma n'\gamma'} = \langle\tilde{\phi}_{n\gamma}|D(E)|\tilde{\phi}_{n'\gamma'}\rangle = [\tilde{D}(E)]_{n'\gamma'n\gamma}$. Since the total current operator J_s is a sum of bond current operators, a result analogous to equation (61) holds for J_s too. This result [36, 99, 104], which the author has referred to as the zero-current theorem in the past, enables us to write equations (58) and (59) as

$$J_{n'n} = \int[f_1(E) - f_2(E)]\,\mathrm{Tr}[\mathrm{J}_{n'n}D_1(E)]\,\mathrm{d}E \tag{62}$$

$$J_S = \int[f_1(E) - f_2(E)]\,\mathrm{Tr}[\mathrm{J}_S D_1(E)]\,\mathrm{d}E. \tag{63}$$

These equations are the basis of the TB transport formalism. We will now use them to derive various alternative expressions for the current in the lead–sample–lead system.

4. Total current and conductance

We will derive five equivalent sets of expressions for the total steady-state electrical current and the differential conductance of the lead–sample–lead system in figure 1. We will begin by showing explicitly that, as may be expected physically, J_S in equation (63) is independent of S. This will give us a starting set of current and conductance formulae, from which all other forms of these quantities may be obtained.

4.1. Fundamental current and conductance formulae

Let us choose two different surfaces open S and S' across the lead–sample–lead system. Let J_S and $J_{S'}$ be the operators for the electron particle current across S and S', respectively. Let, as before, the projection operator $\Delta\mathcal{P} = \mathcal{P}'_1 - \mathcal{P}_1$ contain the sites, finite in number, enclosed between S and S'. As was shown earlier, $D_1(E)$ in equation (49) is independent of the choice of surface, used to define the projection operators in that equation. For equation (49), then, let us select some third surface S''. Let $\mathcal{P}''_1$ and $\mathcal{P}''_2$ be the analogues of $\mathcal{P}_1$ and $\mathcal{P}_2$, defined with respect to S''. Thus, $D_1(E)$ is now given by equation (49) with $\mathcal{P}_1$ and $\mathcal{P}_2$ replaced by $\mathcal{P}''_1$ and $\mathcal{P}''_2$, respectively. Let $D_1(E, \epsilon)$ now be given by equation (51) with $\mathcal{P}_1$ and $\mathcal{P}_2$ replaced by $\mathcal{P}''_1$ and $\mathcal{P}''_2$, respectively. Let S'' be chosen to lie sufficiently far to the left of S and S' to ensure that all sites appearing in ΔP lie to the right of S'', and that no site appearing in ΔP is bonded to any site on the left of S''. Therefore, $\Delta\mathcal{P}\,\mathcal{P}''_1 = \mathcal{P}''_1\,\Delta\mathcal{P} = 0$, $\Delta\mathcal{P}\,\mathcal{H}\mathcal{P}''_1 = \mathcal{P}''_1\mathcal{H}\,\Delta\mathcal{P} = 0$ and $\Delta\mathcal{P}\,\mathcal{P}''_2\mathcal{H}\mathcal{P}''_1 = \mathcal{P}''_1\mathcal{H}\mathcal{P}''_2\,\Delta\mathcal{P} = 0$. Let $\Delta J = J_{S'} - J_S$. Then, after some rearrangement, we find

$$\mathrm{Tr}[\Delta J\, D_1(E, \epsilon)] = -(1/\mathrm{i}\hbar)\,\mathrm{Tr}[(\Delta\mathcal{P}\,\mathcal{H} - \mathcal{H}\,\Delta\mathcal{P})D_1(E, \epsilon)]$$
$$= (1/2\pi\hbar)(z - z^*)\,\mathrm{Tr}[\Delta\mathcal{P}\,G(z)(\mathcal{P}''_2\mathcal{H}\mathcal{P}''_1 - \mathcal{P}''_1\mathcal{H}\mathcal{P}''_2)G(z^*)]. \tag{64}$$

When taken in the positional basis, the trace in the last line above contains only a finite number of terms. Hence, in the limit $\epsilon \to 0^+$, $\mathrm{Tr}[\Delta J\, D_1(E, \epsilon)]$ tends to zero as $(z - z^*) = 2\mathrm{i}\epsilon$. Hence, $\Delta J = \int[(f_1(E) - f_2(E))\,\mathrm{Tr}[\Delta J\, D_1(E)]\,\mathrm{d}E = 0$, and hence

$$J_S = \int [f_1(E) - f_2(E)]\,\mathrm{Tr}[J_S D_1(E)]\,\mathrm{d}E = J_{S'} = \int [f_1(E) - f_2(E)]\,\mathrm{Tr}[J_{S'} D_1(E)]\,\mathrm{d}E.$$
$$\tag{65}$$

Hence, J_S in equations (59) and (63) is independent of the choice of surface S, used to define the current operator J_S. The choice of S in those equations is a matter of convenience.

For any S, the quantity

$$I = eJ_S = e \int [f_1(E) - f_2(E)]\,\mathrm{Tr}[J_S D_1(E)]\,\mathrm{d}E \tag{66}$$

is the steady-state electrical current in the system from figure 1. Equation (66) enables one to compute the current, and derivatives thereof such as the differential conductance $\sigma = \mathrm{d}I/\mathrm{d}W$, in the lead–sample–lead system, at any bias W. In the limit of low bias and low temperature, equation (66) gives the zero-voltage, zero-temperature conductance

$$\sigma_0 = (\mathrm{d}I/\mathrm{d}W)_{W=0} = (I/W)_{W=0} = 2e^2\,\mathrm{Tr}[J_S D_1(E_F)] \tag{67}$$

where a spin-degeneracy factor of 2 has been included, E_F is the Fermi level in the lead–sample–lead system at $W = 0$, and the operator $D_1(E_F)$ is computed at $W = 0$. σ_0 is defined with respect to the applied bias W and gives the conductance between the reservoirs in figure 1 [36].

4.2. Current and conductance formulae with one cutting surface

Our next expression for I uses the set-up in figure 2. Let us take $D_1(E)$ in the form given by equation (36). Using $\mathcal{P}_2\mathcal{H}_0\mathcal{P}_1 = \mathcal{P}_1\mathcal{H}_0\mathcal{P}_2 = 0$, together with equation (23), we may write equation (18) for the current operator J_S as

$$J_S = (1/i\hbar)[\mathcal{P}_2, \mathcal{V}]. \tag{68}$$

Using these results, and using the invariance of the trace under cyclic permutations, we may now write

$$\text{Tr}[J_S D_1(E)] = (1/i\hbar)\,\text{Tr}\{[1 + \mathcal{V}G^-(E)](\mathcal{P}_2\mathcal{V} - \mathcal{V}\mathcal{P}_2)[1 + G^+(E)\mathcal{V}]d_1(E)\}. \tag{69}$$

In view of equations (22), (44) and (45), $g_1(E)g_2(E) = g_2(E)g_1(E) = 0$. This, together with equations (43)–(45), gives

$$\text{Tr}[J_S D_1(E)] = (2\pi/\hbar)\,\text{Tr}[t^\dagger(E)d_2(E)t(E)d_1(E)] \tag{70}$$

where

$$t(E) = \mathcal{V} + \mathcal{V}G^+(E)\mathcal{V}. \tag{71}$$

Therefore, equations (66) and (67) may be written as [4, 36, 38]

$$I = (e/h)4\pi^2 \int [f_1(E) - f_2(E)]\,\text{Tr}[t^\dagger(E)d_2(E)t(E)d_1(E)]\,\mathrm{d}E \tag{72}$$

$$\sigma_0 = (2e^2/h)4\pi^2\,\text{Tr}[t^\dagger(E_F)d_2(E_F)t(E_F)d_1(E_F)]. \tag{73}$$

Let us stress that for a given $\mathcal{H}$—the Hamiltonian of the current-carrying lead–sample–lead system in figure 1—the choice of surface S and of $\mathcal{V}^{(1)}$ and $\mathcal{V}^{(2)}$ in equation (33) is arbitrary, within the specifications given in connection with that equation. If $g^\pm(E)$ in equations (44) and (45) is liked to $G^\pm(E)$ via equation (43), then—for a given $\mathcal{H}$—any S and any $\mathcal{V}$ of the form given in equation (33) will produce the same I in equation (72) and the same σ_0 in equation (73).

4.3. Current and conductance formulae with two cutting surfaces

Let us now select two open surfaces, S and S', with S' to the right of S as shown in figure 3. Let, as before, the projection operators $\mathcal{P}_1$ and $\mathcal{P}_2$ be defined with respect to S, and $\mathcal{P}_1'$ and $\mathcal{P}_2'$ be defined with respect to S'. Let us now perform a cut both along S and along S'. These two cuts may, furthermore, be accompanied by arbitrary modifications to the TB Hamiltonian to the left of S, between S and S', and to the right of S', so long as these modifications involve only a finite number of atomic sites. This may be achieved by writing

$$\mathcal{H} = \bar{\mathcal{H}}_0 + \bar{\mathcal{V}} \tag{74}$$
$$\begin{aligned}\bar{\mathcal{V}} =\ & \mathcal{P}_1\mathcal{H}\mathcal{P}_2 + \mathcal{P}_2\mathcal{H}\mathcal{P}_1 \\ & + \mathcal{P}_1'\mathcal{H}\mathcal{P}_2' + \mathcal{P}_2'\mathcal{H}\mathcal{P}_1' \\ & + \bar{\mathcal{V}}^{(1)} + \Delta\mathcal{V} + \bar{\mathcal{V}}^{(2)}\end{aligned} \tag{75}$$

where a bar is used to avoid confusion with quantities used in the case of a single cut. The terms in the first line of equation (75) contain the bonds intersected by S. The terms in the second line of that equation contain the bonds intersected by S'. Here, we have assumed that there are no bonds intersected by S and S' simultaneously. The Hermitian operators $\bar{\mathcal{V}}^{(1)}$, $\Delta\mathcal{V}$ and $\bar{\mathcal{V}}^{(2)}$ in the third line of equation (75) each have a finite number of non-zero positional matrix elements. $\bar{\mathcal{V}}^{(1)}_{n\gamma n'\gamma'}$ can be non-zero only if both n and n' lie on the left of S, $\Delta\mathcal{V}_{n\gamma n'\gamma'}$ can be non-zero only if both n and n' lie between S and S', and $\bar{\mathcal{V}}^{(2)}_{n\gamma n'\gamma'}$ can be
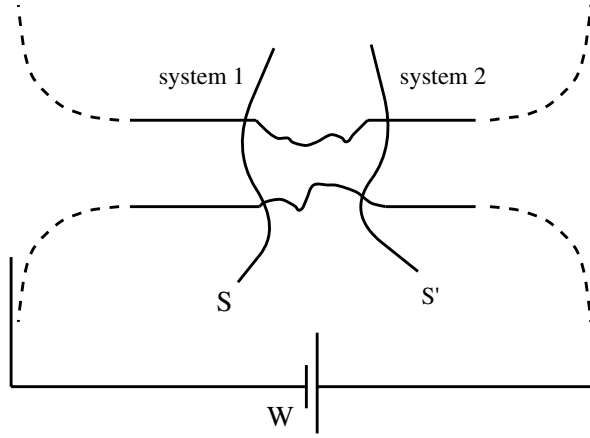
Figure 3. The lead–sample–lead system with two cutting surfaces, S and S'. The semi-infinite systems 1 and 2, on the left of S and on the right of S' respectively, are described by a TB Hamiltonian obtained from the original Hamiltonian for the lead–sample–lead system by the removal of all hopping integrals intersected by S and of all hopping integrals intersected by S', possibly accompanied by arbitrary modifications to a finite number of other hopping integrals and on-site energies. The details are discussed in the text.

non-zero only if both n and n' lie on the right of S'. Within these specifications, $\bar{\mathcal{V}}^{(1)}$, $\Delta\mathcal{V}$ and $\bar{\mathcal{V}}^{(2)}$ are arbitrary. The system described by the Hamiltonian $\bar{\mathcal{H}}_0 = \mathcal{H} - \bar{\mathcal{V}}$ consists of three decoupled systems—the semi-infinite system on the left of S; the finite system between S and S'; and the semi-infinite system on the right of S'. The semi-infinite system on the left of S will now be referred to as system 1, and the semi-infinite system on the right of S' will now be referred to as system 2, as shown in figure 3. Equation (75) is just a special case of equation (33): the terms in the second line of equation (75), grouped together with the second and third term in the third line, constitute a special case of the term $\mathcal{V}^{(2)}$ in equation (33).

The retarded and advanced Green operators, $\bar{g}^{\pm}(E)$, for the system after the cut are related to the Green operators $G^{\pm}(E)$ for the original lead–sample–lead system by

$$G^{\pm}(E) = \bar{g}^{\pm}(E) + \bar{g}^{\pm}(E)\bar{\mathcal{V}}G^{\pm}(E) = \bar{g}^{\pm}(E) + G^{\pm}(E)\bar{\mathcal{V}}\bar{g}^{\pm}(E). \tag{76}$$

Let

$$\bar{g}_1^{\pm}(E) = \mathcal{P}_1\bar{g}^{\pm}(E) = \bar{g}^{\pm}(E)\mathcal{P}_1 \tag{77}$$

$$\bar{g}_2^{\pm}(E) = \mathcal{P}_2'\bar{g}^{\pm}(E) = \bar{g}^{\pm}(E)\mathcal{P}_2' \tag{78}$$

be the retarded and advanced Green operators for systems 1 and 2 in figure 3, respectively [36]. Let

$$2\pi i \bar{d}_1(E) = \bar{g}_1^{-}(E) - \bar{g}_1^{+}(E) \tag{79}$$

$$2\pi i \bar{d}_2(E) = \bar{g}_2^{-}(E) - \bar{g}_2^{+}(E) \tag{80}$$

be the density-of-states operators for the decoupled systems 1 and 2 in figure 3, respectively [36].

In equation (66), let us take $D_1(E)$ in the form given by equation (49). Using $\mathcal{P}_2\bar{\mathcal{H}}_0\mathcal{P}_1 = \mathcal{P}_1\bar{\mathcal{H}}_0\mathcal{P}_2 = 0$, together with equation (23), we may replace $\mathcal{P}_2\mathcal{H}\mathcal{P}_1 - \mathcal{P}_1\mathcal{H}\mathcal{P}_2$ in equation (49) by $\bar{\mathcal{V}}\mathcal{P}_1 - \mathcal{P}_1\bar{\mathcal{V}}$. Using equations (76), (77) and (79), $D_1(E)$ may be cast as $D_1(E) = [1 + G^{+}(E)\bar{\mathcal{V}}]\bar{d}_1(E)[1 + \bar{\mathcal{V}}G^{-}(E)]$. For the current operator in equation (66), let us

now select that across S', $J_{S'}$. Using $\mathcal{P}_2'\bar{\mathcal{H}}_0\mathcal{P}_1' = \mathcal{P}_1'\bar{\mathcal{H}}_0\mathcal{P}_2' = 0$, together with $\mathcal{P}_1' + \mathcal{P}_2' = \mathbf{1}$, we may write $J_{S'} = (1/i\hbar)(\mathcal{P}_2'\mathcal{H}\mathcal{P}_1' - \mathcal{P}_1'\mathcal{H}\mathcal{P}_2') = (1/i\hbar)[\mathcal{P}_2', \bar{\mathcal{V}}]$. Proceeding by analogy with equation (69), we obtain [36]

$$I = (e/h)4\pi^2 \int [f_1(E) - f_2(E)] \, \mathrm{Tr}[\bar{t}^\dagger(E)\bar{d}_2(E)\bar{t}(E)\bar{d}_1(E)] \, \mathrm{d}E \qquad (81)$$

$$\sigma_0 = (2e^2/h)4\pi^2 \, \mathrm{Tr}[\bar{t}^\dagger(E_F)\bar{d}_2(E_F)\bar{t}(E_F)\bar{d}_1(E_F)] \qquad (82)$$

where

$$\bar{t}(E) = \bar{\mathcal{V}} + \bar{\mathcal{V}}G^+(E)\bar{\mathcal{V}}. \qquad (83)$$

For a given $\mathcal{H}$—the Hamiltonian of the current-carrying lead–sample–lead system in figure 1— the choice of S and S', and of $\bar{\mathcal{V}}^{(1)}$, $\Delta\mathcal{V}$ and $\bar{\mathcal{V}}^{(2)}$ in equation (75), is arbitrary, within the specifications given in connection with that equation. If $\bar{g}^\pm(E)$ in equations (77) and (78) is linked to $G^\pm(E)$ via equation (76), then—for a given $\mathcal{H}$—any S and S' and any $\bar{\mathcal{V}}$ of the form given in equation (75) will produce the same I in equation (81) and the same σ_0 in equation (82).

4.4. Kubo form of the current and conductance formulae

Another form of equations (66) and (67) is given by [38]

$$I = (eh/2) \int [f_1(E) - f_2(E)] \, \mathrm{Tr}[J_S D(E) J_S D(E)] \, \mathrm{d}E \qquad (84)$$

$$\sigma_0 = (2e^2/h)(h^2/2) \, \mathrm{Tr}[J_S D(E_F) J_S D(E_F)]. \qquad (85)$$

The choice of surface S in J_S in equations (84) and (85) is again arbitrary, and is a matter of convenience.

To derive equation (84), we once again start from equation (66). Let us take $D_1(E)$ in the form given by equation (49). In J_S, let us select the same, arbitrarily chosen, surface S as that used to define $\mathcal{P}_1$ and $\mathcal{P}_2$ in equation (49). Let us invoke equation (18) to write equation (49) as

$$2\pi i D_1(E) = \mathcal{P}_1 G^-(E) - G^+(E)\mathcal{P}_1 + i\hbar G^+(E) J_S G^-(E). \qquad (86)$$

We also need the following results. First, let us consider the quantity $\mathrm{Tr}[J_S G^+(E) J_S G^+(E)]$. Let us replace $G^+(E)$ inside the trace by $G(z)$, where $z = E + i\epsilon$, with ϵ a small positive real number. Let us write J_S in the form given by equation (20). Then, using equation (25) and taking the limit $\epsilon \to 0^+$, we find

$$i\hbar \, \mathrm{Tr}[J_S G^+(E) J_S G^+(E)] = -\mathrm{Tr}[G^+(E) J_S \mathcal{P}_1] + \mathrm{Tr}[J_S G^+(E)\mathcal{P}_1]. \qquad (87)$$

Let us now invoke the transformed positional basis $\{|\tilde{\phi}_{n\gamma}\rangle\}$, introduced in equation (60), in which $\mathcal{H}$ and $G^\pm(E)$ are symmetric matrices. In that basis, J_S is an antisymmetric matrix. Taking the trace in the basis $\{|\tilde{\phi}_{n\gamma}\rangle\}$, we see that $-\mathrm{Tr}[G^+(E) J_S \mathcal{P}_1] = \mathrm{Tr}[J_S G^+(E)\mathcal{P}_1]$. Hence,

$$i\hbar \, \mathrm{Tr}[J_S G^+(E) J_S G^+(E)] = 2 \, \mathrm{Tr}[J_S G^+(E)\mathcal{P}_1]. \qquad (88)$$

Similarly,

$$i\hbar \, \mathrm{Tr}[J_S G^-(E) J_S G^-(E)] = -2 \, \mathrm{Tr}[J_S \mathcal{P}_1 G^-(E)]. \qquad (89)$$

By similar arguments,

$$\mathrm{Tr}[J_S G^+(E) J_S G^-(E)] = \mathrm{Tr}[J_S G^-(E) J_S G^+(E)]. \qquad (90)$$

The equivalence of equations (66) and (84) follows from equations (31), (86), (88)–(90). The form of equation (85) for the zero-voltage conductance is familiar also from linear-response theory [116]. In equation (84) above, this algebraic form has been generalized to arbitrary voltages.

4.5. Landauer formula

The Landauer formula [117] relates the current in the lead–sample–lead system to the probabilities for electrons incident in lead 1 to be transmitted across the sample region into lead 2. The Landauer formula may be derived from the TB transport formalism as follows.

Let us go back to the set-up in figure 2. Let us consider system 1—the semi-infinite piece on the left after the cut has been made. We stipulated at the start that far from the sample region each lead is a uniform crystalline wire. The most general definition of such a wire is a regular stack of identical unit blocks. The unit block itself can have any size, structure, geometry and composition. Let us consider for a moment an infinite such wire. Its electron eigenstates form a set of bands. The states in each band, $\{|\theta, b\rangle\}$, are travelling Bloch waves along the wire, with a normalization chosen here as one electron per unit block. θ is a dimensionless wavevector along the wire and index b labels the band. The group velocity v_b, in unit blocks per second, and the particle current J_b, carried by state $|\theta, b\rangle$, are, in magnitude, $v_b = J_b = (1/\hbar)|\mathrm{d}E_b/\mathrm{d}\theta|$, where $E_b = E_b(\theta)$ is the band energy in subband b. If a given energy E falls within a given energy subband b, then that subband, or channel, is said to be open at energy E.

Each eigenstate, $|\phi_1\rangle$, of system 1 in figure 2 consists of an incident wave $|\theta_1, b_1\rangle$, backscattered by the severed end. We may thus label $|\phi_1\rangle$ by θ_1 and b_1, $|\phi_1\rangle = |\phi_{\theta_1 b_1}\rangle$, and we may replace $\sum_1$ in equation (38) by $\sum_{b1} \int \mathrm{d}\theta_1/2\pi$. A similar analysis may be made for system 2—the semi-infinite piece on the right after the cut has been made, but we do not need to do this explicitly here. Recalling equations (38) and (39), we may now write

$$4\pi^2 \,\mathrm{Tr}[t^\dagger(E)d_2(E)t(E)d_1(E)] = 4\pi^2 \sum_{1,2} |\langle\phi_2|t(E)|\phi_1\rangle|^2 \delta(E - E_1)\delta(E - E_2)$$

$$= \sum_{b_1 \in \mathrm{open}} T_{b_1}(E) \tag{91}$$

$$T_{b_1}(E) = (2\pi/\hbar)(1/J_{b_1}) \sum_2 |\langle\phi_2|t(E)|\phi_{\theta_1 b_1}\rangle|^2 \delta(E - E_2) \tag{92}$$

where $t(E)$ is given by equation (71), b_1 runs over the open channels in lead 1 at energy E and $E_{b_1}(\theta_1) = E$. From scattering theory, we may identify $T_{b_1}(E)$ above as the total probability that an electron, incident with energy E in channel b_1 in lead 1, will be transmitted across the sample region into lead 2. Equations (72) and (73) can now be written as

$$I = (e/h) \int \mathrm{d}E \, [f_1(E) - f_2(E)] \sum_{b_1 \in \mathrm{open}} T_{b_1}(E) \tag{93}$$

$$\sigma_0 = (2e^2/h) \sum_{b_1 \in \mathrm{open}} T_{b_1}(E_F). \tag{94}$$

Equation (94) is the multichannel Landauer formula for the conductance with respect to the electrochemical potential difference between the reservoirs, $\mu_1 - \mu_2 = eW$ [117].

4.6. Discussion

Above, it was shown that equations (72), (81), (84) and (93) for the total steady-state current, I, in the lead–sample–lead system from figure 1 are algebraically equivalent to equation (66), and are equivalent to one another. Similarly, equations (73), (82), (85) and (94) for the zero-voltage, zero-temperature conductance between the reservoirs, σ_0, are algebraically equivalent to equation (67), and are equivalent to one another. The different appearances of these equations may suggest different respective interpretations. For example, equations (72) and (73) make contact with scattering theory and transmission probabilities, leading to the Landauer formulae

in equations (93) and (94), while equation (85) affords a comparison with linear-response theory. Nonetheless, however varied the interpretations, for a given lead–sample–lead system, specified by a given Hamiltonian $\mathcal{H}$, the five sets of expressions for I and σ_0 derived above are physically and mathematically equivalent.

These five sets of equations for I and σ_0 are used widely in TB conduction calculations, although their derivations can vary. There are two principal reasons for the numerical efficiency and usefulness of these equations. The first is the relatively modest size of TB orbital basis sets in general. The second is that the evaluation of these equations requires knowledge of the Green function for the lead–sample–lead system only over a limited set of atomic sites. In fact, in the case of equations (66) and (84) for I, and the corresponding equations for σ_0, one needs this Green function at a single, arbitrary interface in the system.

As an illustration of the numerical power of the method, references [38] and [39] contain calculations of the resistance as a function of length in disordered three-dimensional quantum wires with cross-sections containing a hundred or more atoms, and with lengths reaching many hundreds of atoms, with configurational averaging over a hundred or more disorder realizations along the way. These calculations enabled a direct study of the transitions between the ballistic, diffusive and localization regimes, and a direct, exact evaluation of the residual resistivity of the respective disordered medium, from the gradient of the resistance as a function of wire length in the diffusive regime. These calculation were performed six years ago on an ordinary workstation without difficulty.

A typical TB transport calculation starts with the evaluation of the Green function on the surfaces of two semi-infinite perfect leads, employing a variety of standard methods [3, 36–39, 78, 84, 87, 88, 99]. Calculations then proceed in various ways, depending on the size of the system. For a small sample region, one may construct and bond the sample region to the leads in one go, by solving the appropriate Dyson equation for the Green function [36, 99]. Alternatively, one may grow the sample slice by slice, starting with a bare lead [3, 38, 39]. The Green function is recalculated on the last added slice at each step, by solving the Dyson equation. This procedure ensures that the calculation scales only linearly with the system length. The growth process may start from one lead and proceed to the other lead, or it may start from both leads simultaneously and continue until the two pieces of the system meet at a chosen interface.

Finally, although the five sets of equations for I and σ_0 above were derived here in the context of TB, the same derivation, the same equations and the same strategies for the evaluation of these equations would hold for a general electronic model on a discrete computational mesh [1–4].

5. Local current and potential

So far, we have considered the calculation of the total current in the lead–sample–lead system, as a function of the applied battery voltage W. We will now consider two further questions: the local spatial distribution of this current and the spatial variation of the self-consistent electron potential in the conducting system. The local current density and local potential in the presence of current flow can provide invaluable insight into the nature and mechanism of current flow and into the concept of resistance at the atomistic scale.

5.1. Local current

Recalling equations (58) and (62), for the electrical bond current from atomic site n' into site n, $I_{n'n}$, we write [99, 104]

$$I_{n'n} = e J_{n'n} = e \, \mathrm{Tr}[\mathrm{J}_{n'n}\Omega(W)] \tag{95}$$

$$= e \int [f_1(E) - f_2(E)] \, \mathrm{Tr}[\mathrm{J}_{n'n}D_1(E)] \, \mathrm{d}E \tag{96}$$

$$= e \, \mathrm{Tr}[\mathrm{J}_{n'n} \, \Delta\Omega] \tag{97}$$

where $\Delta\Omega = \Omega(W) - \Omega(0)$. For equation (97) we have used the fact that at $W = 0$ we have $f_1(E) = f_2(E)$ and hence, from equation (96), $\mathrm{Tr}[\mathrm{J}_{n'n}\Omega(0)] = 0$.

Invoking equation (16), we may also write $I_{n'n}$ as

$$I_{n'n} = (2e/\hbar) \sum_{\gamma,\gamma'} \mathrm{Im}\{\mathcal{H}_{n\gamma n'\gamma'}[\Omega(W)]_{n'\gamma'n\gamma}\} \tag{98}$$

$$= (2e/\hbar) \int [f_1(E) - f_2(E)] \sum_{\gamma,\gamma'} \mathrm{Im}\{\mathcal{H}_{n\gamma n'\gamma'}[D_1(E)]_{n'\gamma'n\gamma}\} \tag{99}$$

$$= (2e/\hbar) \sum_{\gamma,\gamma'} \mathrm{Im}(\mathcal{H}_{n\gamma n'\gamma'} \, \Delta\Omega_{n'\gamma'n\gamma}). \tag{100}$$

In the limit of low bias and low temperature, equation (99) simplifies to

$$I_{n'n} = (4e^2 W/\hbar) \sum_{\gamma,\gamma'} \mathrm{Im}\{\mathcal{H}_{n\gamma n'\gamma'}[D_1(E_F)]_{n'\gamma'n\gamma}\} \tag{101}$$

where, as in equation (67), a spin-degeneracy factor of 2 has been included, E_F is the Fermi level in the lead–sample–lead system at $W = 0$, and the operator $D_1(E_F)$ is computed at $W = 0$.

We will illustrate the use of equation (101) by a model example. We take a simple TB model, with a single spherically symmetric orbital per site on a two-dimensional simple square lattice [104]. Only nearest-neighbour sites are coupled by the TB Hamiltonian. Let us adopt the magnitude of the nearest-neighbour hopping integral as the unit of energy. Let the on-site energy on the native metal atoms at zero bias be chosen as 0. With this choice of energy scale, the conduction band for the infinite perfect simple square lattice extends from -4 to $+4$. If sites n' and n are nearest neighbours, then equation (101) reduces to

$$I_{n'n} = (4e^2 W/\hbar)\mathcal{H}_{n'n} \, \mathrm{Im}[D_1(E_F)]_{n'n} \tag{102}$$

where $\mathcal{H}_{nn'} = \mathcal{H}_{n'n}$ is the nearest-neighbour hopping integral.

The system for our example is shown in figure 4(a). It is a two-dimensional metallic wire with a uniform width of twelve atoms, containing a four-atom-thick insulating region. There are four randomly positioned metal atoms, embedded in the insulator. Figure 4(b) shows the zero-voltage, zero-temperature conductance σ_0, given by equation (67), for this system, as a function of Fermi energy. At most energies, the conductance is much less than the quantum conductance unit, $2e^2/h$. Such low conductances are characteristic of tunnelling. The four conductance peaks, where the conductance rises to values of the order of $2e^2/h$, correspond to resonant transmission.

The physical mechanism of the resonance may be seen pictorially from the nature of the spatial distribution of the current. Figure 5 contains plots of the local current at each of the four conductance resonances from figure 4. The arrow at each atomic site is the vector sum of the bond currents involving that site, divided by two to reflect the fact that each bond current is shared between two sites. We see that at each conductance peak, transmission occurs via a path through the barrier that employs particular metal atoms, embedded in the barrier, as stepping stones. This is an example of resonant transmission through quasibound states. In this case, the quasibound states are the orbitals on the metal atoms in the insulator, slightly split and broadened in energy by the coupling to the leads and to the surrounding barrier atoms. An analogous example, relevant to the field of STM, is resonant transmission through a molecule between two metallic electrodes [118].
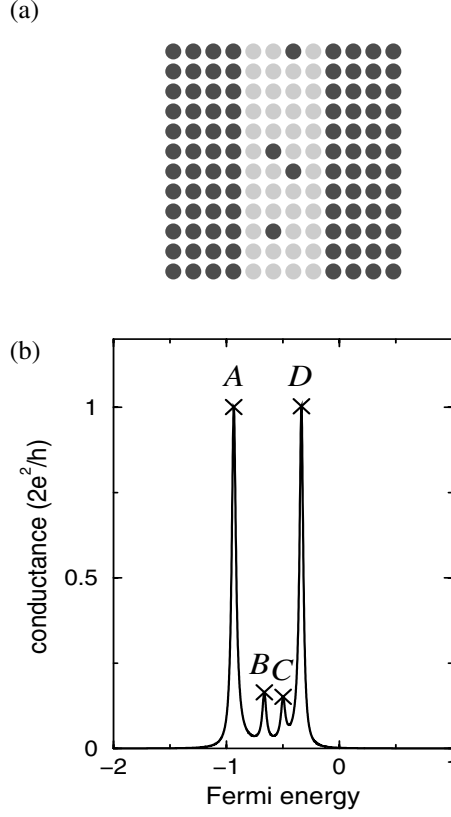
(a)

(b)

Figure 4. (*a*) A segment of a two-dimensional infinitely long twelve-atom-wide conducting wire, containing a four-atom-thick disordered insulating barrier. The dark circles are the native metal atoms, with an on-site energy of zero. The light circles are the insulator atoms, with an on-site energy of +6. The dark circles in the barrier are metal atoms embedded in the insulator. (*b*) The zero-voltage, zero-temperature conductance for this system as a function of the Fermi energy.

5.2. Local potential

Now we turn to the spatial variation of the self-consistent one-electron potential in the current-carrying lead–sample–lead system. In a TB model, the local potential is represented by the diagonal Hamiltonian matrix elements, or on-site energies, $\{\mathcal{H}_{n\gamma n\gamma}\}$. We will see later that in an *ab initio* TB model [103] each on-site energy is given by $\langle\phi_{n\gamma}|(\hat{T}+\hat{V})|\phi_{n\gamma}\rangle$, where $|\phi_{n\gamma}\rangle$ is an actual atomic orbital at site n, $\hat{T}$ is the kinetic energy operator and $\hat{V}=\int|\boldsymbol{r}\rangle V(\boldsymbol{r},t)\langle\boldsymbol{r}|\,\mathrm{d}\boldsymbol{r}$ is the actual self-consistent local one-electron potential. Here, $V(\boldsymbol{r},t)=\delta\mathcal{E}/\delta\rho$, where $\mathcal{E}=\mathcal{E}[\rho]$ is the electrostatic plus the exchange–correlation energy of the electrons, as a functional of the instantaneous electron density at time t, $\rho=\rho(\boldsymbol{r},t)$. Therefore, each on-site energy contains a spatial average of the effective local one-electron potential, weighted by the electron density associated with orbital $|\phi_{n\gamma}\rangle$.

A possible simplification is to assume that at each site n, $\{\mathcal{H}_{n\gamma n\gamma}\}$ can vary at most by a rigid on-site shift, Δ_n, independent of γ [99, 119]. In this simplified picture, Δ_n represents the effective local one-electron potential at site n. In view of the above remarks, this effective potential must, fundamentally, be viewed as the Hartree potential plus an exchange–correlation
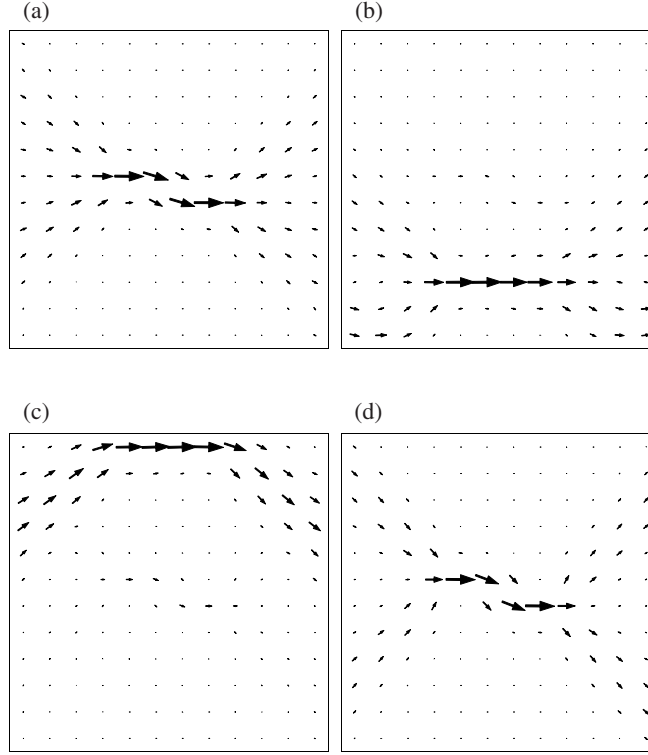
Figure 5. (*a*) The local current at each atomic site at conductance resonance *A* in figure 4, with $E_F = -0.936$. The current is proportional to the length of the arrow. The largest arrow on the plot corresponds to a current of $0.73 \times 2e^2 W/h$. (*b*) The local current at each atomic site at conductance resonance *B* in figure 4, with $E_F = -0.666$. The largest arrow on the plot corresponds to a current of $0.12 \times 2e^2 W/h$. (*c*) The local current at each atomic site at conductance resonance *C* in figure 4, with $E_F = -0.499$. The largest arrow on the plot corresponds to a current of $0.11 \times 2e^2 W/h$. (*d*) The local current at each atomic site at conductance resonance *D* in figure 4, with $E_F = -0.337$. The largest arrow on the plot corresponds to a current of $0.89 \times 2e^2 W/h$.

correction. Ultimately, the on-site energy shifts $\{\Delta_n\}$ must be calculated as self-consistent functions of the electron charge distribution in the system. This must be done by setting up an appropriate TB form of the self-consistent equations that couple the electron density ρ to the effective potential V in calculations based on the Poisson equation or on DFT [32, 109, 111]. Examples of such charge-self-consistent TB transport calculations are given in [57,63,69,120]. Here, we will consider such self-consistent TB models later on, in connection with TD TB and current-induced forces.

A widely used approximation is to adjust $\{\Delta_n\}$ in such a way as to keep the electron occupancy of each site fixed [8, 16, 93–95, 97, 99–102, 119, 121]. We will refer to this approximation as the approximation of LCN. The justification for the LCN approximation, as well as its limitations, must be stated explicitly. In homogeneous regions in a metal, where the one-electron potential varies sufficiently slowly spatially, LCN becomes exact [104]. In such regions $\{\Delta_n\}$, calculated within the LCN approximation, give a correct description of the variation of the self-consistent one-electron potential. In such regions, furthermore, the effective one-electron potential and the electrochemical potential [107] follow each other in shape [104, 109, 122], and hence, up to an additive constant, in such regions the $\{\Delta_n\}$ give also the local electrochemical potential.

In regions of electron scattering, in the vicinity of crystal defects or other structural irregularities or geometrical variations, there may in reality be deviations from LCN. In such regions, and in general, LCN may be justified by appealing to a variational principle. This principle allows a system, both in equilibrium and in the presence of steady-state conduction, to be described by a free-energy function, which is stationary with respect to small variations in the one-electron wavefunctions [99, 119]. The use of the approximate wavefunctions that produce LCN, therefore, should introduce a second-order error into this free-energy function, and into quantities derived from it, such as interatomic forces [99, 119]. Hence, provided that the deviations from LCN that exist in reality are not extreme, LCN may be expected to give a good description of interatomic forces, within the limitations of the TB orbital basis set used. In the case of quantities that are not derived from the variational free-energy function, such as, indeed, the effective one-electron potential or the electron charge density, LCN should be viewed merely as giving a model indication of their spatial variation. An alternative view of LCN as the limit of vanishing capacitance will be discussed later in the paper.

Even within LCN, the calculation of the on-site energy shifts $\{\Delta_n\}$ in general requires an iterative numerical procedure, both in the absence and in the presence of current flow [99]. However, a conceptually transparent and informative approximate expression for the one-electron potential in the presence of current flow may be obtained by the following Thomas–Fermi-type argument [41, 104].

In an orthogonal TB model, the electron occupancy of site n is given by $\text{Tr}[P_n \Omega(W)] = \sum_\gamma [\Omega(W)]_{n\gamma n\gamma}$. Let us, without loss of generality, set $\mu_1 = E_F + eW/2$ and $\mu_2 = E_F - eW/2$, where, once again, μ_1 and $\mu_2 = \mu_1 - eW$ are the electrochemical potentials of reservoirs 1 and 2 in figure 1, respectively, and E_F is the position of the Fermi level in the lead–sample–lead system in the absence of current flow. When the battery is connected, it populates all right-travelling states with energies from E_F up to $\mu_1 = E_F + eW/2$, and it depopulates all left-travelling states with energies from E_F down to $\mu_2 = E_F - eW/2$. To lowest order in W, this changes the electron occupancy of site n by an amount $(eW/2) \sum_\gamma \{[D_1(E_F)]_{n\gamma n\gamma} - [D_2(E_F)]_{n\gamma n\gamma}\}$, per spin. Assume now that the local potential varies sufficiently slowly spatially to ensure that variations in this potential rigidly shift the local band structure. Then, to keep the occupancy of site n fixed, the on-site energy of that site must be shifted by an amount eW_n such that $eW_n \sum_\gamma [D(E_F)]_{n\gamma n\gamma} = (eW/2) \sum_\gamma \{[D_1(E_F)]_{n\gamma n\gamma} - [D_2(E_F)]_{n\gamma n\gamma}\}$, or

$$W_n = (W/2)[(D_1)_n - (D_2)_n]/D_n = W[(D_1)_n/D_n - 1/2] \tag{103}$$

where $(D_1)_n = \sum_\gamma [D_1(E_F)]_{n\gamma n\gamma}$, $(D_2)_n = \sum_\gamma [D_2(E_F)]_{n\gamma n\gamma}$ and $D_n = \sum_\gamma [D(E_F)]_{n\gamma n\gamma} = (D_1)_n + (D_2)_n$. Since the one-electron potential is defined only up to an arbitrary additive constant, we may also write W_n in the symmetric form

$$eW_n = [\mu_1 (D_1)_n + \mu_2 (D_2)_n]/D_n. \tag{104}$$

The bias-induced on-site potential shifts $\{W_n\}$ in equation (103) represent the additional self-consistent one-electron potential that develops in the system upon the onset of steady-state current flow. Equation (103) illustrates two general features of this additional, bias-induced potential profile. First, $0 < (D_1)_n < D_n$ and hence, at any point in the lead–sample–lead system, $|W/2| > W_n > -|W/2|$. Therefore, the potential difference between any two points within the lead–sample–lead system will in general be less in magnitude than the full battery voltage W, which is attained between a point deep in reservoir 1 and a point deep in reservoir 2 [41, 104, 108, 109, 123]. Hence, the conductance between any two points within the lead–sample–lead system in general exceeds the conductance between the reservoirs [41, 104, 108, 109, 123], given by σ_0 in equations (67), (73), (82), (85) and (94).

If the leads have an infinite transverse size compared with the sample region, then deep inside lead 1 the amplitude of the left-travelling states $\{|\psi_2\rangle\}$ tends to zero, because of the

geometrical spreading of the transmitted parts of the left-travelling wavefunctions, as they emerge from the narrow sample region into the left lead. Hence, deep inside lead 1, $(D_2)_n \rightarrow 0$, $(D_1)_n/D_n \rightarrow 1$ and $W_n \rightarrow W/2$. By a similar argument, deep in lead 2, $W_n \rightarrow -W/2$. Hence, as stated earlier, the leads now themselves play the role of reservoirs, and σ_0 in equations (67), (73), (82), (85) and (94) may be viewed as the conductance between a point deep in lead 1 and a point deep in lead 2.

If the leads have a finite cross-section, then there is a limit to how much an electron wave, transmitted through the sample, can spread out in the lead beyond. The transmitted parts of the left-travelling wavefunctions now remain finite in amplitude everywhere in lead 1. Hence, $(D_1)_n/D_n$ now never quite makes it up to unity in lead 1. Therefore, except in the limit of a completely opaque sample, W_n never quite reaches $W/2$ in lead 1, and, by a similar argument, it never quite reaches $-W/2$ in lead 2. Hence, now the conductance between a point in lead 1 and a point in lead 2 will exceed the conductance σ_0 between the reservoirs [41, 104, 108, 109, 123]. Expressions for this enhanced conductance between the leads have been derived explicitly [108, 117].

The second point, shown by equation (103), is that since in defect-free homogeneous regions in a metal the amplitudes of the electron wavefunctions will vary at most through interference oscillations, without net attenuation, in such regions $(D_1)_n$ and D_n, and hence also W_n, will stay constant, apart from interference oscillations. Therefore, in a metal, the potential drops occur in the vicinity of scattering centres and structural and geometrical inhomo-geneities [41, 104, 109, 122, 124, 125], such as defects, interfaces and changes in cross-section.

Equation (103) is a computationally cheap source of qualitative insight, as may be seen by the following model example. We take the same two-dimensional orthonormal nearest-neighbour TB model as that used for figures 4 and 5 above. The system now is a metallic wire with a uniform width of 31 atoms, containing a section with five randomly distributed substitutional impurities. At zero bias, the on-site energy on the native metal atoms is once again set to zero, and it is set to +4 on the impurity atoms. The Fermi level at zero bias is $E_F = -1$, close to the middle of the band. We now turn on the battery bias W between the reservoirs in figure 1, and use equation (103) to calculate the resulting on-site potential shifts $\{W_n\}$ in the wire. Since a single type of orbital is present in the model, in equation (103) now $(D_1)_n = [D_1(E_F)]_{nn}$, $(D_2)_n = [D_2(E_F)]_{nn}$ and $D_n = [D(E_F)]_{nn}$.

Figure 6(a) shows W_n at each atom in the segment of the wire containing the impurities. The impurities are represented by the ringed circles. A contour plot of the same data is shown in figure 6(b). There is a net potential drop across the disordered wire segment[1]. However, this drop is not a uniform potential ramp, but is highly inhomogeneous. We see a concentrated, localized potential drop across each impurity, with gentler potential variations in the defect-free regions between the impurities. The potential profile across each defect has a characteristic bipolar form, called a resistivity dipole. The concept of the resistivity dipole was introduced by Landauer nearly half a century ago [124]. This concept has since then been studied by many authors, for example in [41, 104, 109, 122, 125–134]. Panels (c) and (d) in figure 6 show $\{W_n\}$ after averaging over 200 impurity configurations with the same impurity concentration as in panels (a) and (b). It is only after the configurational averaging that the one-electron potential drop in the disordered wire segment begins to assume the form of a uniform ramp. The reduction, in magnitude, in the extreme values of the potential, relative to the case before the averaging, is due to the disappearance of the dramatic localized dipoles. Figure 6 demonstrates a key property of metallic conduction: the potential drops, and the corresponding electric field,

---

[1] As may be expected from the foregoing discussion, the potential drop across the disordered wire segment is less than the full battery voltage W.
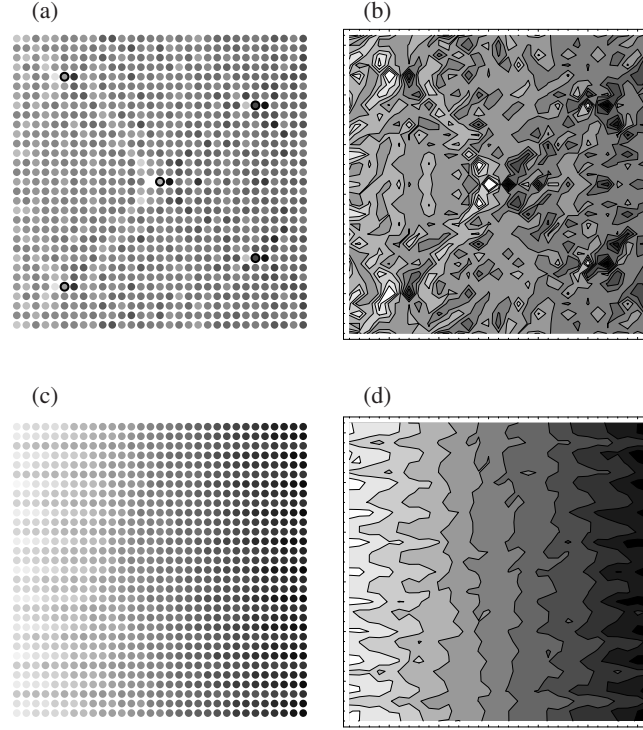
Figure 6. (*a*) The bias-induced on-site potential shifts in a 31-atom-long segment of an infinite 31-atom-wide current-carrying wire, containing five impurities. Each impurity is marked by a bold ring around the respective circle. The lightest shading on the plot corresponds to a potential of $0.28\,W$ and the darkest shading to $-0.24\,W$, where W is the battery bias. (*b*) The data from panel (*a*) as a contour plot. (*c*) The bias-induced on-site potential shifts after averaging over 200 configurations with the same impurity concentration as in panel (*a*). The lightest shading on the plot corresponds to $0.08\,W$ and the darkest shading to $-0.08\,W$. (*d*) The data from panel (*c*) as a contour plot.

in a current-carrying disordered metal are concentrated in the vicinity of the scattering centres, through the formation of resistivity dipoles [122, 124, 125]. At the atomistic scale every defect acts as an elemental resistor.

6. Current-induced forces

The applied voltages in nanojunction transport experiments can exceed 1 V, resulting in enormous local current densities. Even without detailed calculation, one may expect significant additional forces on atoms to develop under these conditions, resulting in significant changes in the mechanical properties and stability of nanoscale conductors [135]. Recently, a generalization of the TB bond model [119] to current-carrying systems has been developed [99]. This formalism allows intrinsic interatomic forces, the electrical current and current-induced forces in a nanojunction to be computed in a single internally consistent calculation. This formalism has been used to calculate interatomic forces in the presence of current and to find the activation barriers and rates for current-induced atomistic processes, such as electromigration and current-induced fracture of atomic wires [99, 101, 102]. Reference [72] gives an application of the TB force expression from [99] to current-induced forces on adsorbates in carbon nanotubes.

The limitations of the formalism in [99] are that it was derived under steady-state conditions, it uses the LCN approximation and it ignores the overlap of atomic orbitals on neighbouring atoms. These limitations may be overcome by a TD generalization of TB, which describes dynamically and self-consistently an interacting system of quantum electrons and classical nuclei [103]. In this section, we will obtain the general form of the dynamical TB equations [103]. Under steady-state conditions, in the limit of LCN, we will recover the expression for interatomic forces in the presence of current flow from [99]. We will generalize this steady-state force expression beyond orthogonal TB and beyond LCN.

6.1. Time-dependent Lagrangian mean-field theory

The derivation of the dynamical TB equations starts from a TD Lagrangian mean-field theory, describing the motion of an interacting set of N_e quantum electrons and N_z classical nuclei. In this mean-field theory, the energy of the electron–electron interaction, at any time t, is represented by a functional, $\mathcal{E}_{hxc} = \mathcal{E}_{hxc}[\rho]$, of the instantaneous electron density $\rho = \rho(r, t)$. We will not consider spin-dependent interactions. The choice of $\mathcal{E}_{hxc}$ is a specification of the theory. Within the Hartree approximation, $\mathcal{E}_{hxc}$ would be given by the Hartree energy. In an improved approximation, $\mathcal{E}_{hxc}$ might be given by the Hartree energy plus the exchange–correlation energy, calculated from ground-state DFT in the local density approximation [136, 137]. Here, we treat $\mathcal{E}_{hxc}[\rho]$ as a general differentiable model functional.

The dynamical equations of the theory may be obtained from the Lagrangian [103, 137]

$$L = i\hbar \sum_{i=1}^{N_e} \langle \psi_i(t)|\dot{\psi}_i(t)\rangle - \sum_{i=1}^{N_e} \langle \psi_i(t)|\hat{T}|\psi_i(t)\rangle - \mathcal{E}[\rho] + \sum_{n=1}^{N_z} M_n [\dot{R}_n(t)]^2/2 - \phi[\{R_n(t)\}]$$

(105)

where

$$\mathcal{E}[\rho] = \sum_{n=1}^{N_z} \int \rho(r, t) v_n[r - R_n(t)]\, dr + \mathcal{E}_{hxc}[\rho]$$

(106)

$$\rho = \rho(r, t) = \sum_{i=1}^{N_e} |\psi_i(r, t)|^2.$$

(107)

Here, $\{|\psi_i(t)\rangle\}$ is a set of N_e one-particle states, one for each electron in the system, and $\psi_i(r, t) = \langle r|\psi_i(t)\rangle$. $\hat{T} = \hat{p}^2/2m_e$ is the one-electron kinetic energy operator, where $\hat{p}$ is the one-particle momentum operator. We recall the property $\langle r|\hat{p}|r'\rangle = -i\hbar \nabla \delta(r - r')$. Throughout the paper, $\nabla = (\partial/\partial x, \partial/\partial y, \partial/\partial z)$ with $r = (x, y, z)$. $R_n(t)$, $\dot{R}_n(t)$ and M_n are the position, velocity and mass of nucleus n, respectively. Everywhere below $\dot{F} = dF/dt$ and $\ddot{F} = d^2F/dt^2$, for any function of time $F = F(t)$. ϕ is the nucleus–nucleus interaction potential and v_n is the interaction potential between an electron and nucleus n. Everywhere index i refers to electrons and index n refers to nuclei. From now on, the limits in summations over these indices will be omitted, on the understanding that in such summations i runs from 1 to N_e, and n runs from 1 to N_z. In equation (105), and everywhere from now on, the inner product $\langle \eta|\zeta\rangle$ is defined by

$$\langle \eta|\zeta\rangle = \int \langle \eta|r\rangle\, dr\, \langle r|\zeta\rangle$$

(108)

for any two one-particle states $|\eta\rangle$ and $|\zeta\rangle$.

Let us write $|\psi_i(t)\rangle = \sum_\zeta \psi_{i\zeta}(t)|\zeta\rangle$ and $|\dot\psi_i(t)\rangle = \sum_\zeta \dot\psi_{i\zeta}(t)|\zeta\rangle$, where $\{|\zeta\rangle\}$ is an arbitrary complete orthonormal time-independent one-electron basis. The Lagrangian in equation (105) becomes[2]

$$L = L(\{\psi_{i\zeta}\}, \{\dot\psi_{i\zeta}\}, \{\psi_{i\zeta}^*\}, \{\dot\psi_{i\zeta}^*\}, \{\boldsymbol{R}_n\}, \{\dot{\boldsymbol{R}}_n\})$$

$$= i\hbar \sum_{i,\zeta} \psi_{i\zeta}^* \dot\psi_{i\zeta} - \sum_{i,\zeta,\zeta'} \psi_{i\zeta}^* T_{\zeta\zeta'} \psi_{i\zeta'} - \mathcal{E}[\rho] + \sum_n M_n \dot{\boldsymbol{R}}_n^2/2 - \phi(\{\boldsymbol{R}_n\}) \qquad (109)$$

where $\psi_{i\zeta} = \psi_{i\zeta}(t)$, $\boldsymbol{R}_n = \boldsymbol{R}_n(t)$, $T_{\zeta\zeta'} = \langle\zeta|\hat{T}|\zeta'\rangle$ and $\rho = \rho(\boldsymbol{r},t) = \sum_{i,\zeta,\zeta'} \psi_{i\zeta}^*(t)\langle\zeta|\boldsymbol{r}\rangle\langle\boldsymbol{r}|\zeta'\rangle\psi_{i\zeta'}(t)$. The Lagrangian equations of motion are [103][3]

$$\partial L/\partial\psi_{i\zeta} - (\mathrm{d}/\mathrm{d}t)(\partial L/\partial\dot\psi_{i\zeta}) = 0 \qquad (110)$$

$$\partial L/\partial\psi_{i\zeta}^* - (\mathrm{d}/\mathrm{d}t)(\partial L/\partial\dot\psi_{i\zeta}^*) = 0 \qquad (111)$$

$$\partial L/\partial\boldsymbol{R}_n - (\mathrm{d}/\mathrm{d}t)(\partial L/\partial\dot{\boldsymbol{R}}_n) = 0. \qquad (112)$$

Equation (111) yields the one-electron TD SE

$$i\hbar\dot\psi_{i\zeta}(t) = \sum_{\zeta'} H_{\zeta\zeta'}\psi_{i\zeta'}(t) \qquad (113)$$

where

$$H_{\zeta\zeta'} = \langle\zeta|\hat{H}|\zeta'\rangle \qquad \hat{H} = \hat{T} + \hat{V} \qquad \hat{V} = \int |\boldsymbol{r}\rangle V(\boldsymbol{r},t)\langle\boldsymbol{r}|\,\mathrm{d}\boldsymbol{r} \qquad (114)$$

$$V(\boldsymbol{r},t) = \delta\mathcal{E}[\rho]/\delta\rho = \sum_n v_n[\boldsymbol{r} - \boldsymbol{R}_n(t)] + v_{hxc}(\boldsymbol{r},t) \qquad v_{hxc}(\boldsymbol{r},t) = \delta\mathcal{E}_{hxc}[\rho]/\delta\rho. \quad (115)$$

Equation (110) gives the complex conjugate of equation (113). In evaluating equations (110) and (111), we have used the relation

$$\partial\mathcal{E}/\partial\psi_{i\zeta}^* = \int (\delta\mathcal{E}/\delta\rho)(\partial\rho/\partial\psi_{i\zeta}^*)\,\mathrm{d}\boldsymbol{r} = \sum_{\zeta'} \int \langle\zeta|\boldsymbol{r}\rangle V(\boldsymbol{r},t)\langle\boldsymbol{r}|\zeta'\rangle\psi_{i\zeta'}(t)\,\mathrm{d}\boldsymbol{r}$$

$$= \sum_{\zeta'} \langle\zeta|\hat{V}|\zeta'\rangle\psi_{i\zeta'}(t) = (\partial\mathcal{E}/\partial\psi_{i\zeta})^*. \qquad (116)$$

Equation (112) gives

$$M_n\ddot{\boldsymbol{R}}_n(t) = -\int \rho(\boldsymbol{r},t)\boldsymbol{\nabla}_n v_n[\boldsymbol{r} - \boldsymbol{R}_n(t)]\,\mathrm{d}\boldsymbol{r} - \boldsymbol{\nabla}_n\phi \qquad (117)$$

where $\boldsymbol{\nabla}_n = (\partial/\partial R_{nx}, \partial/\partial R_{ny}, \partial/\partial R_{nz})$ with $\boldsymbol{R}_n = \boldsymbol{R}_n(t) = (R_{nx}, R_{ny}, R_{nz})$. We will refer to equation (117), and to analogous Newtonian equations of motion, generically as the Hellmann–Feynman (HF) theorem. The energy of the system is given by the Legendre transformation

$$E = \sum_{i,\zeta} \dot\psi_{i\zeta}(\partial L/\partial\dot\psi_{i\zeta}) + \sum_{i,\zeta} \dot\psi_{i\zeta}^*(\partial L/\partial\dot\psi_{i\zeta}^*) + \sum_n \dot{\boldsymbol{R}}_n \cdot (\partial L/\partial\dot{\boldsymbol{R}}_n) - L \qquad (118)$$

$$= \sum_i \langle\psi_i(t)|\hat{T}|\psi_i t\rangle + \mathcal{E}[\rho] + \sum_n M_n[\dot{\boldsymbol{R}}_n(t)]^2/2 + \phi[\{\boldsymbol{R}_n(t)\}]. \qquad (119)$$

In may verified directly that equations (113) and (117) conserve the orthonormality of electron states and the total energy and momentum of the system of electrons and nuclei [103, 137].

---

[2] In the present case $\dot\psi_{i\zeta}^*$ does not appear in L, but it is accommodated in the formalism for generality.

[3] In this Lagrangian procedure, the real and imaginary parts of $\psi_{i\zeta}$ must be treated as independent variables. This is equivalent to treating $\psi_{i\zeta}$ and $\psi_{i\zeta}^*$ as independent variables [103].

6.2. Time-dependent tight binding

TD TB results from an exact rearrangement of the quantity $\mathcal{E}$ in equation (106), combined with a particular choice of basis, namely an atomic orbital basis. Let us first make the following modifications. For generality, we replace the bare nuclei by ions, although we may equally well adhere to an all-electron description. Now v_n in equation (106) is the ionic pseudopotential of ion n, and ϕ in equation (105) is the ion–ion interaction potential. M_n, $\boldsymbol{R}_n(t)$ and $\dot{\boldsymbol{R}}_n(t)$ are now the mass, position and velocity of ion n, respectively. The N_e electrons that appear explicitly in the theory are the valence electrons, described by a set of N_e one-particle states $\{|\psi_i(t)\rangle\}$. The density ρ in equation (107) now is the valence-electron density. The choice of $\mathcal{E}_{hxc}[\rho]$ in equation (106) is once again a specification of the theory.

Next, we imagine performing a self-consistent valence-electron calculation for atom n in isolation, placed at position $\boldsymbol{R}_n(t)$. This calculation produces a set of atomic orbitals $\{|\phi_{n\gamma}\rangle\}$, normalized to unity, with occupation numbers $\{f_{n\gamma}\}$. Index γ labels the various orbitals on atom n. The numbers $\{f_{n\gamma}\}$ are constants. Let

$$\langle r|\phi_{n\gamma}\rangle = \phi_{n\gamma}[\boldsymbol{r} - \boldsymbol{R}_n(t)] \tag{120}$$

be the orbital wavefunction, corresponding to state $|\phi_{n\gamma}\rangle$. Then

$$\rho_n = \rho_n[\boldsymbol{r} - \boldsymbol{R}_n(t)] = \sum_\gamma f_{n\gamma} |\phi_{n\gamma}[\boldsymbol{r} - \boldsymbol{R}_n(t)]|^2 \tag{121}$$

is the valence-electron density of atom n in isolation. Let

$$\rho_0 = \rho_0[\boldsymbol{r}, \{\boldsymbol{R}_n(t)\}] = \sum_n \rho_n[\boldsymbol{r} - \boldsymbol{R}_n(t)]. \tag{122}$$

ρ_0 is a rigid superposition of atomic valence-electron densities.

We now write the quantity $\mathcal{E}[\rho]$ in equation (106) as

$$\mathcal{E}[\rho] = \mathcal{E}[\rho_0] + \int \{\rho(\boldsymbol{r}, t) - \rho_0[\boldsymbol{r}, \{\boldsymbol{R}_n(t)\}]\} V_0(\boldsymbol{r}, t) \, \mathrm{d}\boldsymbol{r} + \mathcal{E}^{TB}[\rho]$$
$$V_0(\boldsymbol{r}, t) = (\delta\mathcal{E}/\delta\rho)_{\rho=\rho_0}. \tag{123}$$

V_0 is the effective potential V in equation (115), evaluated at electron density ρ_0. The density functional $\mathcal{E}^{TB}[\rho]$ is defined by equation (123). If $\mathcal{E}^{TB}[\rho]$ has a convergent Taylor expansion, then it may be approximated by a finite series in powers of $\Delta\rho(\boldsymbol{r}, t) = \rho(\boldsymbol{r}, t) - \rho_0[\boldsymbol{r}, \{\boldsymbol{R}_n(t)\}]$ as follows [103]:

$$\mathcal{E}^{TB}[\rho] \approx \sum_{k=2}^{M} (1/k!) \int \Delta\rho(\boldsymbol{r_1}, t) \cdots \Delta\rho(\boldsymbol{r_k}, t) F_k(\boldsymbol{r_1}, \ldots, \boldsymbol{r_k}) \, \mathrm{d}\boldsymbol{r_1} \cdots \mathrm{d}\boldsymbol{r_k}. \tag{124}$$

Here, $F_k(\boldsymbol{r_1}, \ldots, \boldsymbol{r_k}) = [\delta^k \mathcal{E}_{hxc}/\delta\rho(\boldsymbol{r_1}, t) \cdots \delta\rho(\boldsymbol{r_k}, t)]_{\rho=\rho_0}$, and M defines the order of the approximation. $M = 2$ would correspond to the functionals used in [138] and [139].

Using equation (123), we may write

$$\sum_i \langle \psi_i(t)|\hat{T}|\psi_i(t)\rangle + \mathcal{E}[\rho] = \sum_i \langle \psi_i(t)|\hat{H}^0|\psi_i(t)\rangle$$
$$- \sum_{n,\gamma} f_{n\gamma} \langle \phi_{n\gamma}|\hat{H}^0|\phi_{n\gamma}\rangle + \mathcal{E}^{TB}[\rho] + \Delta\mathcal{E} + C \tag{125}$$

where

$$\hat{H}^0 = \hat{T} + \hat{V}_0 \qquad \hat{V}_0 = \int |\boldsymbol{r}\rangle V_0(\boldsymbol{r}, t)\langle \boldsymbol{r}| \, \mathrm{d}\boldsymbol{r} \tag{126}$$

$$C = \sum_n (T_n + \mathcal{E}_n) \tag{127}$$

$$\Delta\mathcal{E} = \mathcal{E}[\rho_0] - \sum_n \mathcal{E}_n. \tag{128}$$

Here, $T_n = \sum_\gamma f_{n\gamma} \langle \phi_{n\gamma} | \hat{T} | \phi_{n\gamma} \rangle$ is the kinetic energy of the valence electrons in atom n in isolation, and is a constant. $\mathcal{E}_n = \int \rho_n[r - R_n(t)] v_n[r - R_n(t)] \, dr + \mathcal{E}_{hxc}[\rho_n]$ is the electrostatic and exchange–correlation energy of atom n in isolation, and is a constant. C is a sum of electronic energies of free atoms, and is a constant. $\Delta \mathcal{E} = \Delta \mathcal{E}[\{R_n(t)\}]$ is a function only of the ionic positions. Equation (125) is exact, apart from a possible finite-order approximation to $\mathcal{E}^{TB}$, as in equation (124). Equation (125) serves as the basis for TD TB.

We now make the defining step in the derivation of the TD TB equations, and force the electron states $\{|\psi_i(t)\rangle\}$ to be linear combinations of the atomic orbitals $\{|\phi_{n\gamma}\rangle\}$ by writing [103]

$$|\psi_i(t)\rangle = \sum_{n,\gamma} \psi_{n\gamma}^i(t) |\phi_{n\gamma}\rangle \tag{129}$$

$$|\dot{\psi}_i(t)\rangle = \sum_{n,\gamma} [\dot{\psi}_{n\gamma}^i(t) |\phi_{n\gamma}\rangle + \psi_{n\gamma}^i(t) |\dot{\phi}_{n\gamma}\rangle]. \tag{130}$$

Here, $|\dot{\phi}_{n\gamma}\rangle = |\nabla_n \phi_{n\gamma}\rangle \cdot \dot{R}_n(t)$, where $|\nabla_n \phi_{n\gamma}\rangle$ is defined by $\langle r|\nabla_n \phi_{n\gamma}\rangle = \nabla_n \langle r|\phi_{n\gamma}\rangle$. The valence-electron density in equation (107) becomes

$$\rho = \rho(r, t) = \sum_{i,n,\gamma,n',\gamma'} \psi_{n\gamma}^{i*}(t) \phi_{n\gamma}^*[r - R_n(t)] \phi_{n'\gamma'}[r - R_{n'}(t)] \psi_{n'\gamma'}^i(t). \tag{131}$$

Let us define

$$Q_{n\gamma n'\gamma'} = \langle \phi_{n\gamma} | \nabla_{n'} \phi_{n'\gamma'} \rangle = -\langle \phi_{n\gamma} | \nabla \phi_{n'\gamma'} \rangle = (1/i\hbar) \langle \phi_{n\gamma} | \hat{p} | \phi_{n'\gamma'} \rangle \tag{132}$$

where $|\nabla \phi_{n'\gamma'}\rangle$ is defined by $\langle r|\nabla \phi_{n'\gamma'}\rangle = \nabla \langle r|\phi_{n'\gamma'}\rangle$. Let us introduce the Hermitian matrices

$$H_{n\gamma n'\gamma'}^0 = \langle \phi_{n\gamma} | \hat{H}^0 | \phi_{n'\gamma'} \rangle \tag{133}$$

$$S_{n\gamma n'\gamma'} = \langle \phi_{n\gamma} | \phi_{n'\gamma'} \rangle. \tag{134}$$

Finally, let

$$\Omega_{n'\gamma'n\gamma} = \sum_i \psi_{n'\gamma'}^i(t) \psi_{n\gamma}^{i*}(t) \tag{135}$$

$$\Omega_{n'\gamma'n\gamma}^0 = \delta_{nn'} \delta_{\gamma\gamma'} f_{n\gamma}. \tag{136}$$

In the approximation of orthogonal orbitals, the Hermitian density matrix $\Omega_{n'\gamma'n\gamma}$ above corresponds to the matrix $[\Omega(W)]_{n\gamma n'\gamma'}$, used in sections 2–5.

The Lagrangian in equation (105) can now be written as

$$
\begin{aligned}
L^{TB} = {} & L^{TB}(\{\psi_{n\gamma}^i\}, \{\dot{\psi}_{n\gamma}^i\}, \{\psi_{n\gamma}^{i*}\}, \{\dot{\psi}_{n\gamma}^{i*}\}, \{R_n\}, \{\dot{R}_n\}) \\
= {} & i\hbar \sum_{n,\gamma,n',\gamma'} \Omega_{n'\gamma'n\gamma} Q_{n\gamma n'\gamma'} \cdot \dot{R}_{n'} + i\hbar \sum_{i,n,\gamma,n',\gamma'} \psi_{n\gamma}^{i*} S_{n\gamma n'\gamma'} \dot{\psi}_{n'\gamma'}^i \\
& - \sum_{n,\gamma,n',\gamma'} (\Omega_{n'\gamma'n\gamma} - \Omega_{n'\gamma'n\gamma}^0) H_{n\gamma n'\gamma'}^0 - \mathcal{E}^{TB}[\rho] \\
& + \sum_n M_n \dot{R}_n^2/2 - \phi^{TB}(\{R_n\}) - C
\end{aligned}
\tag{137}
$$

where $\psi_{n\gamma}^i = \psi_{n\gamma}^i(t)$, $R_n = R_n(t)$, ρ is given by equation (131) and

$$\phi^{TB}(\{R_n\}) = \phi(\{R_n\}) + \Delta \mathcal{E}(\{R_n\}). \tag{138}$$

ϕ^{TB} is the change in electrostatic and exchange–correlation energy as the free atoms are brought together and rigidly superimposed from infinity, and is an *a priori* function of the atomic species and their positions [99, 103, 119]. ϕ^{TB} can be approximated by a repulsive pair potential [99, 103, 119]. Before deriving the equations of motion from L^{TB}, we now make an aside to extend the derivation to TB models with empirical parameters.

6.3. Empirical tight binding

Above, it was shown how the quantities appearing in the Lagrangian L^{TB} in equation (137) are to be obtained from first principles. However, in practice one may wish to make model assumptions about these quantities. It is therefore desirable to keep the dynamical TB equations open to such empirical models. This is possible, because all derivations, starting from equation (137), require only certain algebraic properties of the quantities $S_{n\gamma n'\gamma'}$, $Q_{n\gamma n'\gamma'}$, $H^0_{n\gamma n'\gamma'}$, $\mathcal{E}^{TB}$, ϕ^{TB} and $\Omega^0_{n'\gamma'n\gamma}$. These properties are the following [103].

(i) The overlap matrix $S_{n\gamma n'\gamma'}$ is Hermitian. For $n \neq n'$, for given γ and γ', $S_{n\gamma n'\gamma'}$ depends only on $(R_n - R_{n'})$, whence $\nabla_n S_{n\gamma n'\gamma'} + \nabla_{n'} S_{n\gamma n'\gamma'} = 0$. $S_{n\gamma n\gamma'}$ is independent of R_n. The overlap matrix is positive definite, in the sense that

$$\sum_{n,\gamma,n',\gamma'} \psi^*_{n\gamma} S_{n\gamma n'\gamma'} \psi_{n'\gamma'} > 0 \tag{139}$$

for any set of numbers $\{\psi_{n\gamma}\}$ that are not all equal to zero[4]. This property guarantees a positive-definite norm for the electron states. It guarantees also that the eigenvalues of the overlap matrix are positive definite and that this matrix is invertible.

(ii) $Q_{n\gamma n'\gamma'}$ satisfies

$$Q_{n\gamma n'\gamma'} = \nabla_{n'} S_{n\gamma n'\gamma'} = -\nabla_n S_{n\gamma n'\gamma'} = -\nabla_n S^*_{n'\gamma'n\gamma} = -Q^*_{n'\gamma'n\gamma} \qquad n \neq n' \tag{140}$$

$$Q_{n\gamma n\gamma'} = -Q^*_{n\gamma'n\gamma} \tag{141}$$

$Q_{n\gamma n\gamma'}$ is independent of R_n.

(iii) The matrix $H^0_{n\gamma n'\gamma'}$ is Hermitian. $H^0_{n\gamma n'\gamma'}$ is a function only of the ionic positions $\{R_n\}$. $H^0_{n\gamma n'\gamma'}$ is invariant under rigid translations of the ions as a whole, whence $\sum_{n''} \nabla_{n''} H^0_{n\gamma n'\gamma'} = 0$.

(iv) $\mathcal{E}^{TB} = \mathcal{E}^{TB}(\{\psi^i_{n\gamma}\}, \{\psi^{i*}_{n\gamma}\}, \{R_n\})$ is such that

$$\partial \mathcal{E}^{TB}/\partial \psi^{i*}_{n\gamma} = \sum_{n',\gamma'} V^{TB}_{n\gamma n'\gamma'} \psi^i_{n'\gamma'} = (\partial \mathcal{E}^{TB}/\partial \psi^i_{n\gamma})^* \tag{142}$$

where $V^{TB}_{n\gamma n'\gamma'}$ is Hermitian. For given $\{\psi^i_{n\gamma}\}$, $\mathcal{E}^{TB}$ is invariant under the transformation $\{R_n\} \to \{R_n + \Delta\}$, for any Δ. Hence, $\nabla_n \mathcal{E}^{TB} = (\partial \mathcal{E}^{TB}/\partial R_n)_{\{\psi^i_{m\gamma}\},\{\psi^{i*}_{m\gamma}\},\{R_{m \neq n}\}}$ satisfies $\sum_n \nabla_n \mathcal{E}^{TB} = 0$. If we are deriving our TB model from first principles, then, by analogy with equation (116), $V^{TB}_{n\gamma n'\gamma'} = \langle \phi_{n\gamma}|\hat{V}^{TB}|\phi_{n'\gamma'}\rangle$, where $\hat{V}^{TB} = \int |r\rangle V^{TB}(r, t)\langle r| \, dr$, $V^{TB}(r, t) = \delta \mathcal{E}^{TB}[\rho]/\delta\rho$, with ρ given by equation (131).

(v) ϕ^{TB} is a function only of the ionic positions $\{R_n\}$. ϕ^{TB} is invariant under rigid translations of the ions as a whole, whence $\sum_n \nabla_n \phi^{TB} = 0$.

(vi) $\{f_{n\gamma}\}$ in equation (136) are constants. C is an arbitrary constant.

All derivations from this point onward rely only on these properties.

---

[4] If, as in equation (134), an overlap matrix $S_{\alpha\alpha'}$ is derived explicitly from a finite set of normalizable functions $\{\phi_\alpha(r)\}$ via $S_{\alpha\alpha'} = \int \phi^*_\alpha(r)\phi_{\alpha'}(r) \, dr$, then this matrix is guaranteed to be positive definite, provided that the functions $\{\phi_\alpha(r)\}$ are linearly independent, in the sense that $\psi(r) = \sum_\alpha \psi_\alpha \phi_\alpha(r) = 0$, $\forall r$, implies $\psi_\alpha = 0$, $\forall \alpha$. Indeed, if the $\{\phi_\alpha(r)\}$ are linearly independent, then for any set of numbers $\{\psi_\alpha\}$ that are not all equal to zero,

$$\sum_{\alpha,\alpha'} \psi^*_\alpha S_{\alpha\alpha'} \psi_{\alpha'} = \int \sum_{\alpha,\alpha'} \psi^*_\alpha \phi^*_\alpha(r)\phi_{\alpha'}(r)\psi_{\alpha'} \, dr = \int |\psi(r)|^2 \, dr > 0$$

$$\psi(r) = \sum_\alpha \psi_\alpha \phi_\alpha(r).$$

.

6.4. Lagrangian equations of motion

The Lagrangian equations of motion, corresponding to L^{TB} in equation (137), are given by equations (110)–(112), with L replaced by L^{TB} and with $\psi_{i\zeta}$ and $\psi_{i\zeta}^*$ replaced by $\psi_{n\gamma}^i$ and $\psi_{n\gamma}^{i*}$, respectively. Equation (111) yields the TD SE

$$i\hbar \sum_{n',\gamma'} Q_{n\gamma n'\gamma'} \cdot \dot{\boldsymbol{R}}_{n'}(t)\psi_{n'\gamma'}^i(t) + i\hbar \sum_{n',\gamma'} S_{n\gamma n'\gamma'} \dot{\psi}_{n'\gamma'}^i(t) = \sum_{n',\gamma'} H_{n\gamma n'\gamma'}^{TB}\psi_{n'\gamma'}^i(t) \tag{143}$$

where

$$H_{n\gamma n'\gamma'}^{TB} = H_{n\gamma n'\gamma'}^0 + V_{n\gamma n'\gamma'}^{TB}. \tag{144}$$

$V_{n\gamma n'\gamma'}^{TB}$ is given by equation (142). Equation (110) gives the complex conjugate of equation (143). In the approximation of orthogonal orbitals, the TB Hamiltonian matrix $H_{n\gamma n'\gamma'}^{TB}$ corresponds to the matrix $\mathcal{H}_{n\gamma n'\gamma'}$, used in sections 2–5. In an *ab initio* TB model, we would have $H_{n\gamma n'\gamma'}^{TB} = \langle \phi_{n\gamma}|(\hat{T} + \hat{V})|\phi_{n'\gamma'}\rangle$ with $\hat{V} = \int |\boldsymbol{r}\rangle V(\boldsymbol{r}, t)\langle \boldsymbol{r}|\,\mathrm{d}\boldsymbol{r}$, where $V(\boldsymbol{r}, t) = V_0(\boldsymbol{r}, t) + V^{TB}(\boldsymbol{r}, t) = \delta\mathcal{E}[\rho]/\delta\rho$ is the effective potential V in equation (115), evaluated at the electron density in equation (131).

The third Lagrangian equation gives the HF theorem

$$\begin{aligned}
M_n\ddot{\boldsymbol{R}}_n(t) = &-\sum_{n',\gamma',n'',\gamma''}(\Omega_{n''\gamma''n'\gamma'} - \Omega_{n''\gamma''n'\gamma'}^0)\boldsymbol{\nabla}_n H_{n'\gamma'n''\gamma''}^0 - \boldsymbol{\nabla}_n\mathcal{E}^{TB} - \boldsymbol{\nabla}_n\phi^{TB} \\
&-\sum_{\gamma,n',\gamma',n'',\gamma'',n''',\gamma'''}(\boldsymbol{Q}_{n\gamma n'\gamma'}S_{n'\gamma'n''\gamma''}^{-1}H_{n''\gamma''n'''\gamma'''}^{TB}\Omega_{n'''\gamma'''n\gamma} + \mathrm{c.c.}) \\
&-i\hbar\sum_{\gamma,n',\gamma'}[\Omega_{n'\gamma'n\gamma}\dot{\boldsymbol{R}}_{n'}(t)\cdot\boldsymbol{\nabla}_{n'}\boldsymbol{Q}_{n\gamma n'\gamma'} - \mathrm{c.c.}] \\
&+i\hbar\sum_{\gamma,n',\gamma',n'',\gamma'',n''',\gamma'''}\{\boldsymbol{Q}_{n\gamma n'\gamma'}S_{n'\gamma'n''\gamma''}^{-1}[\boldsymbol{Q}_{n''\gamma''n'''\gamma'''}\cdot\dot{\boldsymbol{R}}_{n'''}(t)]\Omega_{n'''\gamma'''n\gamma} - \mathrm{c.c.}\}
\end{aligned} \tag{145}$$

where $\boldsymbol{\nabla}_n\mathcal{E}^{TB} = (\partial\mathcal{E}^{TB}/\partial\boldsymbol{R}_n)_{\{\psi_{m\gamma}^i\},\{\psi_{m\gamma}^{i*}\},\{\boldsymbol{R}_{m\neq n}\}}$. For the energy of the system, a Legendre transformation as in equation (118) gives

$$\begin{aligned}
E^{TB} = &\sum_{n,\gamma,n',\gamma'}(\Omega_{n'\gamma'n\gamma} - \Omega_{n'\gamma'n\gamma}^0)H_{n\gamma n'\gamma'}^0 + \mathcal{E}^{TB}[\{\psi_{n\gamma}^i(t)\}, \{\psi_{n\gamma}^{i*}(t)\}, \{\boldsymbol{R}_n(t)\}] \\
&+\sum_n M_n[\dot{\boldsymbol{R}}_n(t)]^2/2 + \phi^{TB}[\{\boldsymbol{R}_n(t)\}] + C.
\end{aligned} \tag{146}$$

Subject to a given set of initial conditions, specifying $\{\psi_{n\gamma}^i(t)\}$, $\{\boldsymbol{R}_n(t)\}$ and $\{\dot{\boldsymbol{R}}_n(t)\}$ at some time, equations (143) and (145) produce unique values for these variables at any later time. Subject to the limitations of treating the ions as classical particles [103], these equations define a dynamical description of the system of electrons and ions. In this description, the electrons are not confined to an instantaneous stationary state. These equations can be used to model conduction and forces on ions away from the steady state and in the presence of a dynamical exchange of energy between the electrons and the ions. A generalization of the *ab initio* semi-classical Lagrangian dynamical formalism, in an orbital basis set, to include an external laser field is given in [140].

It may be verified explicitly [103] that equations (143) and (145) conserve the inner product $\sum_{n,\gamma,n',\gamma'}\psi_{n\gamma}^{i*}(t)S_{n\gamma n'\gamma'}\psi_{n'\gamma'}^j(t)$, the total energy of the system E^{TB} and the quantity

$$P = i\hbar\sum_{n,\gamma,n',\gamma'}Q_{n\gamma n'\gamma'}\Omega_{n'\gamma'n\gamma} + \sum_n M_n\dot{\boldsymbol{R}}_n(t). \tag{147}$$

In view of equation (132), in a first-principles TB scheme the quantity $i\hbar \sum_{n,\gamma,n',\gamma'} Q_{n\gamma n'\gamma'} \Omega_{n'\gamma'n\gamma}$ above may be identified as the total electron momentum $P_e(t) = \sum_i \langle \psi_i(t)|\hat{p}|\psi_i(t)\rangle$. Then conservation of P constitutes conservation of the total mechanical momentum of the system of electrons and ions. In an empirical TB model, $S_{n\gamma n'\gamma'}$ and $Q_{n\gamma n'\gamma'}$ are 'user-defined' parameters. In that case, the extent to which the quantity $i\hbar \sum_{n,\gamma,n',\gamma'} Q_{n\gamma n'\gamma'} \Omega_{n'\gamma'n\gamma}$ may be taken to represent $P_e(t)$ depends on how physical the assumed form of $S_{n\gamma n'\gamma'}$ is. In all cases, however, P in equation (147) is a conserved quantity in the theory.

All terms in equation (145) that involve the matrix $Q_{n\gamma n'\gamma'}$ are Pulay-like forces [141]. Some of these terms depend explicitly on the instantaneous ionic velocities. These velocity-dependent forces do not contribute to the rate of change, $\sum_n M_n \dot{R}_n(t) \cdot \ddot{R}_n(t)$, of the total kinetic energy of the ions [103]. Stated differently, the total work done by these forces is zero. However, these velocity-dependent terms are needed to conserve the quantity P in equation (147) [103, 140].

6.5. Quasistationary ions

We will now subject equations (143) and (145) to a series of approximations. In doing so, ultimately we will recover the steady-state expression for current-induced forces in the charge-neutral model of [99]. The first approximation is that the ionic velocities, $\{\dot{R}_n(t)\}$, are sufficiently small to enable us to ignore all velocity-dependent terms in equations (143) and (145). Then these equations become

$$i\hbar \sum_{n',\gamma'} S_{n\gamma n'\gamma'} \dot{\psi}^i_{n'\gamma'}(t) = \sum_{n',\gamma'} H^{TB}_{n\gamma n'\gamma'} \psi^i_{n'\gamma'}(t) \tag{148}$$

$$M_n \ddot{R}_n(t) = - \sum_{n',\gamma',n'',\gamma''} (\Omega_{n''\gamma''n'\gamma'} - \Omega^0_{n''\gamma''n'\gamma'}) \nabla_n H^0_{n'\gamma'n''\gamma''} - \nabla_n \mathcal{E}^{TB} - \nabla_n \phi^{TB}$$
$$- \sum_{\gamma,n',\gamma',n'',\gamma'',n''',\gamma'''} (Q_{n\gamma n'\gamma'} S^{-1}_{n'\gamma'n''\gamma''} H^{TB}_{n''\gamma''n'''\gamma'''} \Omega_{n'''\gamma'''n\gamma} + \text{c.c.}). \tag{149}$$

The electron wavefunctions $\{\psi^i_{n\gamma}(t)\}$ in these equations do not yet have to satisfy any stationarity conditions. These wavefunctions may, for instance, be a set of wavepackets, describing a set of excess electrons, released from one end of a long molecule with slowly moving or static ions, propagating down the molecule to meet a set of holes, coming up from the other end. In the approximation of orthogonal orbitals, equation (148) reduces to equation (10).

6.6. Quasistationary electrons

Our next assumption is that, at least locally in some region of interest, at some time t, the electron wavefunctions $\psi^i_{n\gamma} = \psi^i_{n\gamma}(t)$ satisfy a time-independent SE of the form

$$\sum_{n',\gamma'} H^{TB}_{n\gamma n'\gamma'} \psi^i_{n'\gamma'} = E_i \sum_{n',\gamma'} S_{n\gamma n'\gamma'} \psi^i_{n'\gamma'} \tag{150}$$

where, as before, $H^{TB}_{n\gamma n'\gamma'} = H^0_{n\gamma n'\gamma'} + V^{TB}_{n\gamma n'\gamma'}$ with $V^{TB}_{n\gamma n'\gamma'}$ given by equation (142). Equation (150) is satisfied exactly, and globally, if the electron subsystem is in a true stationary state of the instantaneous ionic positions [103]. In a closed periodic system, the electron subsystem may carry a current even in such stationary situations. For example, the one-electron eigenstates of a finite ring, consisting of a periodically repeated unit block, may be chosen such as to carry a circular current [99].

We may imagine also situations in which the electrons, without being in global stationary states, have settled into a transient, but long-lived steady state. An example of such a

situation is a capacitor, consisting of two large but finite chunks of metal, undergoing a slow discharge through a thin connecting wire. We considered this scenario earlier, as a possible practical realization of the system in figure 1. Although the current-carrying electrons are not in global eigenstates of the capacitor as a whole, in the region of the connecting wire, locally, these electrons may reasonably be described by the time-independent right- and left-travelling wavefunctions, discussed in section 2, which satisfy a time-independent SE equation like equation (150). Indeed, under steady-state conduction in a nanojunction between two electrodes, the right- and left-travelling wavefunctions in section 2 constitute an explicit form for the quasistationary electron wavefunctions in equation (150), at least in the vicinity of the nanojunction.

The solutions to equation (150) are self-consistent in the sense that they return the same $V_{n\gamma n'\gamma'}^{TB}$, via equation (142), as appears in equation (150). In an actual calculation for a current-carrying nanojunction between two leads, these steady-state wavefunctions would have to be computed self-consistently, using an explicit form for the interaction energy $\mathcal{E}^{TB}$ in equation (142). A simple model form for this energy is discussed below. If, furthermore, the TB parameters are derived from first principles, as outlined in section 6.2, then the calculation would constitute an *ab initio* TB analogue of the DFT method of [111]. The simplest form of self-consistency, namely the imposition of LCN, was used in [99, 101, 102] to calculate the electronic structure and interatomic forces in current-carrying metallic nanojunctions. Examples of *ab initio* TB transport calculations may be found in [71, 72, 113].

As stated above, in a long-lived but transient steady-state process, equation (150) may hold locally, but not necessarily globally. However, if we assume that $Q_{n\gamma n'\gamma'}$, $S_{n'\gamma'n''\gamma''}^{-1}$ and $H_{n''\gamma''n'''\gamma'''}^{TB}$ are sufficiently short ranged to ensure that equation (150) holds within all ionic sites appearing in the last term in equation (149)[5], then we may cast equation (149) as

$$M_n\ddot{\boldsymbol{R}}_n(t) = -\sum_{n',\gamma',n'',\gamma''}(\Omega_{n''\gamma''n'\gamma'} - \Omega_{n''\gamma''n'\gamma'}^0)\boldsymbol{\nabla}_n H_{n'\gamma'n''\gamma''}^0 - \boldsymbol{\nabla}_n\mathcal{E}^{TB} - \boldsymbol{\nabla}_n\phi^{TB}$$

$$+ \sum_{n',\gamma',n'',\gamma''}\Omega_{n''\gamma''n'\gamma'}^E\boldsymbol{\nabla}_n S_{n'\gamma'n''\gamma''} \qquad \Omega_{n''\gamma''n'\gamma'}^E = \sum_i \psi_{n''\gamma''}^i E_i \psi_{n'\gamma'}^{i*} \qquad (151)$$

with $\boldsymbol{\nabla}_n\mathcal{E}^{TB} = (\partial\mathcal{E}^{TB}/\partial\boldsymbol{R}_n)_{\{\psi_{m\gamma}^i\},\{\psi_{m\gamma}^{i*}\},\{\boldsymbol{R}_{m\neq n}\}}$. Equation (151) is a generalization of the force expression in the presence of steady-state conduction from [99] beyond orthogonal TB and beyond LCN.

6.7. Orthogonal self-consistent tight binding

Our next approximation is to impose orthogonality by choosing the overlap matrix as

$$S_{n\gamma n'\gamma'} = \delta_{nn'}\delta_{\gamma\gamma'}. \qquad (152)$$

---

[5] The matrix $Q_{n\gamma n'\gamma'}$, whose off-site elements are derived from those of the matrix $S_{n\gamma n'\gamma'}$ via equation (140), will share the range of the matrix $S_{n\gamma n'\gamma'}$, which, like that of the matrix $H_{n\gamma n'\gamma'}^{TB}$, may reasonably be assumed to be limited. The spatial range of the matrix $S_{n\gamma n'\gamma'}^{-1}$ may be estimated as follows. Let us write $S_{n\gamma n'\gamma'} = \delta_{nn'}\delta_{\gamma\gamma'} - (-\delta S_{n\gamma n'\gamma'})$. The pure off-diagonal matrix $(-\delta S_{n\gamma n'\gamma'})$ has the mathematical properties of a Hamiltonian matrix in orthogonal TB with zero on-site energies. Since, by assumption, the matrix S is positive definite, the eigenvalues of the matrix $(-\delta S)$ must all be less than 1. Hence, the matrix S^{-1} has the mathematical properties of a TB Green function, $(E-H)^{-1}$, with the matrix $(-\delta S)$ playing the role of the TB Hamiltonian matrix H, and with an energy $E = 1$ that lies above the highest eigenvalue of H. If we take the size of our system to infinity, then we may expect the eigenvalues of $(-\delta S)$ to form a continuous band, or bands, all lying below 1. Hence, for such extended systems, $S_{n\gamma n'\gamma'}^{-1}$ must behave like a TB Green function at an energy outside any band, above the uppermost band edge. Therefore, in regions where that Green function decays with distance, so too must $S_{n\gamma n'\gamma'}^{-1}$. In particular, where that Green function decays exponentially with distance, so too must $S_{n\gamma n'\gamma'}^{-1}$.

For purposes of illustration, let us now consider possible model forms for the other ingredients of the TB model. We make every simplification in $H^0_{n\gamma n'\gamma'}$. If $\gamma \neq \gamma'$, then $H^0_{n\gamma n\gamma'} = 0$, while $H^0_{n\gamma n\gamma}$ is a constant independent of the ionic positions, and is a parameter of the model. For $n \neq n'$, for given γ and γ', the hopping integral $H^0_{n\gamma n'\gamma'}$ is a function only of $(\boldsymbol{R}_{n'} - \boldsymbol{R}_n)$, and is a parameter of the model [99, 100]. ϕ^{TB} is approximated by a repulsive pair potential [99, 100, 119].

For $\mathcal{E}^{TB} = \mathcal{E}^{TB}(\{\psi^i_{n\gamma}\}, \{\psi^{i*}_{n\gamma}\}, \{\boldsymbol{R}_n\})$ we take the model expression

$$\mathcal{E}^{TB} = (1/2) \sum_n U_n \, \Delta q_n^2 + (1/2) \sum_n \sum_{n' \neq n} f_{nn'} \, \Delta q_n \, \Delta q_{n'} \qquad \Delta q_n = q_n - q_n^0. \tag{153}$$

Here, $q_n^0 = \sum_\gamma f_{n\gamma}$ is the number of valence electrons in atom n in isolation and $q_n = \sum_\gamma \Omega_{n\gamma n\gamma}$ is the number of valence electrons at site n in our actual system of electrons and ions. Thus, Δq_n is the excess number of electrons at site n. U_n is a constant, independent of the ionic positions. The quantity $f_{nn'} = f_{n'n}$ is a function only of the distance between ions n and n'. U_n and $f_{nn'}$ are parameters of the model [120, 138]. $\mathcal{E}^{TB}$ represents a set of second-order Coulomb-like interactions. This model may be viewed as a monopole version of the multipole self-consistent TB model in [138]. This model may be viewed also as a generalization of the charge-neutral TB bond model in [99, 100] with an explicit inclusion of second-order interaction terms.

$V^{TB}_{n\gamma n'\gamma'}$ in equation (142) is diagonal and is given by

$$V^{TB}_{n\gamma n'\gamma'} = \delta_{nn'} \delta_{\gamma\gamma'} \, \Delta_n \qquad \Delta_n = \left(U_n \, \Delta q_n + \sum_{n'' \neq n} f_{nn''} \, \Delta q_{n''} \right). \tag{154}$$

In this model, variations in the on-site energy $H^{TB}_{n\gamma n\gamma} = H^0_{n\gamma n\gamma} + V^{TB}_{n\gamma n\gamma}$ arise solely from the interaction energy $\mathcal{E}^{TB}$, via $V^{TB}_{n\gamma n\gamma} = \Delta_n$. The on-site energy shifts $\{\Delta_n\}$ in equation (154) constitute an explicit, self-consistent form for the rigid shifts $\{\Delta_n\}$, discussed in section 5.2.

The quantity $\boldsymbol{\nabla}_n \mathcal{E}^{TB}$, appearing in equations (145), (149) and (151), is given by

$$\boldsymbol{\nabla}_n \mathcal{E}^{TB} = (\partial \mathcal{E}^{TB} / \partial \boldsymbol{R}_n)_{\{\psi^i_{m\gamma}\}, \{\psi^{i*}_{m\gamma}\}, \{\boldsymbol{R}_{m \neq n}\}} = \sum_{n' \neq n} \Delta q_n \, \Delta q_{n'} \, \boldsymbol{\nabla}_n f_{nn'}. \tag{155}$$

Equation (151) for the steady-state Newtonian force on ion n now becomes

$$M_n \ddot{\boldsymbol{R}}_n(t) = -2 \sum_{n' \neq n} \sum_{\gamma, \gamma'} \mathrm{Re}(\Omega_{n'\gamma'n\gamma} \boldsymbol{\nabla}_n H^0_{n\gamma n'\gamma'}) - \boldsymbol{\nabla}_n \mathcal{E}^{TB} - \boldsymbol{\nabla}_n \phi^{TB} \tag{156}$$

with $\boldsymbol{\nabla}_n \mathcal{E}^{TB}$ given by equation (155). Equation (156) is a generalization of the force expression in the presence of steady-state conduction from [99] beyond LCN.

6.8. Local charge neutrality

Let us now consider the limit of strong electron–electron repulsion, where $\{U_n\}$ and $\{f_{nn'}\}$ become very large. This limit corresponds to making the capacitance of the system very small. In this limit, the system cannot tolerate the accumulation of excess charges. Hence, in this limit the system will behave in such a way as to keep $\{\Delta q_n\}$ in equation (153) close to zero. This limit, therefore, is the limit of LCN.

Physically, in this limit the on-site energy shifts $\{\Delta_n\}$ in equation (154) should remain finite. Looked at from a numerical point of view, $\Delta q_n \to 0$ must in general be achievable with finite $\{\Delta_n\}$. But if $\{\Delta_n\}$, linear in $\{U_n\}$, $\{f_{nn'}\}$ and linear in $\{\Delta q_n\}$, remain finite, then the quantity $\boldsymbol{\nabla}_n \mathcal{E}^{TB}$ in equation (155), which is linear in $\{U_n\}$, $\{f_{nn'}\}$ and quadratic in $\{\Delta q_n\}$, must tend to zero.

In an actual steady-state calculation in the LCN limit, the $\{V_{n\gamma n\gamma}^{TB} = \Delta_n\}$ are no longer determined by equation (154). Instead, they are adjusted to be such that the solutions to equation (150), with $S_{n\gamma n'\gamma'} = \delta_{nn'}\delta_{\gamma\gamma'}$, give $\Delta q_n = q_n - q_n^0 = 0$. This is done by an iterative numerical procedure. The practical implementation of this procedure for a current-carrying nanojunction is discussed for instance in [99]. Let now $\Omega_{n'\gamma'n\gamma}^{LCN}$ designate the TB density matrix $\Omega_{n'\gamma'n\gamma}$, constructed from the respective solutions to equation (150). Since, as argued above, $\nabla_n \mathcal{E}^{TB} \to 0$ in the LCN limit, and since $V_{n\gamma n'\gamma'}^{TB}$ is diagonal, equation (156) may be written as

$$M_n \ddot{\boldsymbol{R}}_n(t) = -2 \sum_{n' \neq n} \sum_{\gamma,\gamma'} \text{Re}(\Omega_{n'\gamma'n\gamma}^{LCN} \boldsymbol{\nabla}_n H_{n\gamma n'\gamma'}^{TB}) - \boldsymbol{\nabla}_n \phi^{TB} \qquad (157)$$

where, once again, $H_{n\gamma n'\gamma'}^{TB} = H_{n\gamma n'\gamma'}^0 + V_{n\gamma n'\gamma'}^{TB}$. Equation (157) is the force expression in the presence of steady-state conduction, obtained in [99]. In that reference, this expression was obtained from a statistical analysis. Here, it has been derived as the steady-state limit of the general dynamical HF theorem in equation (145), in an orthogonal TB model, in the limit of strong electron–electron repulsions.

7. Summary and future challenges

In this paper, we have discussed the TB approach to the modelling of the mechanical and electronic properties of current-carrying nanoscale systems. Five equivalent sets of expressions for the current and the zero-voltage conductance were derived from scratch. The way in which the current density and self-consistent local potential enter the TB formalism was discussed. In section 6, we derived from first principles a set of coupled TB equations of motion, namely equations (143) and (145), to describe dynamically and self-consistently a set of interacting electrons and ions. The form of the TB Lagrangian in equation (137) allows a range of TB models—from *ab initio* to empirical ones, from the LCN limit of strong electron–electron repulsion to the limit of non-interacting electrons [103]—to be treated within a common framework. The TD formalism opens up the possibility of using TB to model dynamical transport processes, such as the discharge of two initially charged nanoscale clusters connected by an atomic wire, or the propagation of an electron–hole pair in a long molecule. By taking a series of limits, we then recovered an earlier expression for interatomic forces in the presence of steady-state conduction, and we generalized this steady-state force expression beyond LCN and beyond orthogonal TB.

Current-induced mechanical effects in atomic-scale conductors are an attractive recent line of work in the area. Calculations, based on the steady-state force expression from [99], have shown that current flow can result in a dramatic reduction in the strength and stability of atomic wires [102]. These calculations have emphasized furthermore that in order to have a complete picture of current-induced mechanical processes in nanojunctions, it is necessary to know the local temperature in the junction in the presence of current flow [102, 142].

The linear dimension of a nanojunction is typically much smaller than the inelastic electron mean free path. Therefore, individual electrons dissipate only a small fraction of their energy in the junction itself. However, due to the high local current density, there are a lot of current-carrying electrons, each dropping a small part of its energy, in the nanojunction at any one time. Hence, although most of the *global* power may be expected to be dissipated in the nearby macroscopic electrodes [142, 143], the power *per atom* in the nanojunction, where the current density is huge, may be large.

Quantitatively, a simple TB model of electron–phonon coupling suggests that at the current densities, attainable in metallic nanojunctions, the power per atom in the nanojunction can be sufficiently high to lead to a significant local temperature rise [102, 142]. Experimental

evidence for such heating is discussed in [142]. The calculations in [142], however, were based on severe approximations, in which every atom was treated as if it were embedded in a bulk environment. To make further progress it is necessary to devise a model of energy exchange between current-carrying electrons and phonons, combined with thermal conduction away from the nanojunction, that takes account of the local electronic structure and vibrational modes in a realistic nanojunction geometry. One line of approach to this challenge might be the semiclassical dynamical TB formalism in section 6. Another, which would retain the quantum nature of atomic vibrations, may be to extend the TB model of electron–phonon coupling from [142] to incorporate the local electronic and phononic structure in a general atomistic environment. Such atomistic TB simulations of local heating, combined with the TB methods for the simulation of current flow and current-induced forces discussed earlier, would provide a comprehensive unified technique for simulating what happens in current-carrying nanostructures.

Acknowledgments

References

[1] Baranger H U and Stone A D 1989 *Phys. Rev.* B **40** 8169
[2] Baranger H U, DiVincenzo D P, Jalabert R A and Stone A D 1991 *Phys. Rev.* B **44** 10 637
[3] Pendry J B, Pretre A, Rous P J and Martin-Moreno L 1991 *Surf. Sci.* **244** 160
[4] Pendry J B, Pretre A and Krutzen B C H 1991 *J. Phys.: Condens. Matter* **3** 4313
[5] Martin-Rodero A, Flores F and March N H 1988 *Phys. Rev.* B **38** 10 047
[6] Ferrer J, Martin-Rodero A and Flores F 1988 *Phys. Rev.* B **38** 10 113
[7] Mingo N, Jurczyszyn L, Garcia-Vidal F J, Saiz-Pardo R, de Andres P L, Flores F, Wu S Y and More W 1996 *Phys. Rev.* B **54** 2225
[8] Vazquez de Parga A L, Hernan O S, Miranda R, Levy Yeyati A, Mingo N, Martin-Rodero A and Flores F 1988 *Phys. Rev. Lett.* **80** 357
[9] Sautet P and Joachim C 1991 *Chem. Phys. Lett.* **185** 23
[10] Carlisle C I, King D A, Bocquet M-L, Cerda J and Sautet P 2000 *Phys. Rev. Lett.* **84** 3899
[11] Mujica V, Kemp M and Ratner M 1994 *J. Chem. Phys.* **101** 6856
[12] Koetter E, Drakova D and Doyen G 1996 *Phys. Rev.* B **53** 16 595
[13] McKinnon B A and Choy T C 1996 *Phys. Rev.* B **54** 11 777
[14] Cerda J, van Hove M A, Sautet P and Salmeron M 1997 *Phys. Rev.* B **56** 15 885
[15] Cerda J, Yoon A, van Hove M A, Sautet P, Salmeron M and Somorjai G A 1997 *Phys. Rev.* B **56** 15 900
[16] Nieminen J A and Paavilainen S 1998 *Surf. Sci.* **405** L573
[17] Briggs G A D and Fisher A J 1999 *Surf. Sci. Rep.* **33** 1
[18] Sautet P and Joachim C 1988 *Chem. Phys. Lett.* **153** 511
[19] Sautet P and Joachim C 1988 *Phys. Rev.* B **38** 12 238
[20] Joachim C and Vinuesa J F 1996 *Europhys. Lett.* **33** 635
[21] Pizzagalli L, Joachim C, Bouju X and Girard Ch 1997 *Europhys. Lett.* **38** 97
[22] Magoga M and Joachim C 1997 *Phys. Rev.* B **56** 4722
[23] Magoga M and Joachim C 1998 *Phys. Rev.* B **57** 1820
[24] Magoga M and Joachim C 1999 *Phys. Rev.* B **59** 16 011
[25] Kemp M, Mujica V and Ratner M A 1994 *J. Chem. Phys.* **101** 5172
[26] Mujica V, Kemp M and Ratner M A 1994 *J. Chem. Phys.* **101** 6849
[27] Kemp M, Roitberg A, Mujica V, Wanta T and Ratner M A 1996 *J. Phys. Chem.* **100** 8349
[28] Mujica V, Kemp M, Roitberg A and Ratner M A 1996 *J. Chem. Phys.* **104** 7296
[29] Yaliraki S N and Ratner M A 1998 *J. Chem. Phys.* **109** 5036
[30] Yaliraki S N, Kemp M and Ratner M A 1999 *J. Am. Chem. Soc.* **121** 3428
[31] Mujica V, Nitzan A, Mao Y, Davis W, Kemp M, Roitberg A and Ratner M A 1999 *Adv. Chem. Phys.* **107** 403
[32] Mujica V, Roitberg A E and Ratner M 2000 *J. Chem. Phys.* **112** 6834
[33] Samanta M P, Tian W, Datta S, Henderson J I and Kubiak C P 1996 *Phys. Rev.* B **53** 7626
[34] Tian W, Datta S, Hong S, Reifenberger R, Henderson J I and Kubiak C P 1998 *J. Chem. Phys.* **109** 2874
[35] Hall L E, Reimers J R, Hush N S and Silverbrook K 2000 *J. Chem. Phys.* **112** 1510

[36] Todorov T N, Briggs G A D and Sutton A P 1993 *J. Phys.: Condens. Matter* **5** 2389
[37] Todorov T N and Briggs G A D 1994 *J. Phys.: Condens. Matter* **6** 2559
[38] Todorov T N 1996 *Phys. Rev.* B **54** 5801
[39] Todorov T N 1997 *Nanowires* ed P A Serena and N Garcia (Dordrecht: Kluwer)
[40] White C W and Todorov T N 1998 *Nature* **393** 240
[41] Todorov T N 2000 *J. Phys.: Condens. Matter* **12** 8995
[42] Nikolic K and MacKinnon A 1993 *Phys. Rev.* B **47** 6555
[43] Nikolic K and MacKinnon A 1994 *Phys. Rev.* B **50** 11 008
[44] Oakeshott R B S and MacKinnon A 1994 *J. Phys.: Condens. Matter* **6** 1315
[45] Garcia-Mochales P, Serena P A, Garcia N and Costa-Krämer J L 1996 *Phys. Rev.* B **53** 10 268
[46] Garcia-Mochales P and Serena P A 1997 *Phys. Rev. Lett.* **79** 2316
[47] Chico L, Benedict L X, Louie S G and Cohen M L 1996 *Phys. Rev.* B **54** 2600
[48] Tamura R and Tsukada M 1997 *Solid State Commun.* **101** 601
[49] Yevtushenko O M, Slepyan G Ya, Maksimenko S A, Lakhtakia A and Romanov D A 1997 *Phys. Rev. Lett.* **79** 1102
[50] Meunier V and Lambin Ph 1998 *Phys. Rev. Lett.* **81** 5588
[51] Anantram M P and Govindan T R 1998 *Phys. Rev.* B **58** 4882
[52] Kostyrko T, Bartkowiak M and Mahan G D 1999 *Phys. Rev.* B **60** 10 735
[53] Nardelli M B 1999 *Phys. Rev.* B **60** 7828
[54] Treboux G, Lapstun P and Silverbrook K 1999 *Chem. Phys. Lett.* **306** 402
[55] Choi H J and Ihm J 1999 *Solid State Commun.* **111** 385
[56] Rochefort A, Avouris P, Lesage F and Salahub D R 1999 *Phys. Rev.* B **60** 13 824
[57] Farajan A A, Esfarjani K and Kawazoe Y 1999 *Phys. Rev. Lett.* **82** 5084
[58] Maksimenko A S and Slepyan G Ya 2000 *Phys. Rev. Lett.* **84** 362
[59] Sanvito S, Kwon Y-K, Tomanek D and Lambert C J 2000 *Phys. Rev. Lett.* **84** 1974
[60] Nakanishi T, Igami M and Ando T 2000 *Physica* E **6** 872
[61] Wakabayashi K and Sigrist M 2000 *Phys. Rev. Lett.* **84** 3390
[62] Orlikowski D, Nardelli M B, Bernholc J and Roland C 2000 *Phys. Rev.* B **61** 14 194
[63] Leonard F and Tersoff J 2000 *Phys. Rev. Lett.* **85** 4767
[64] Anantram M P, Datta S and Xue Y 2000 *Phys. Rev.* B **61** 14 219
[65] Roland C, Nardelli M B, Wang J and Guo H 2000 *Phys. Rev. Lett.* **84** 2921
[66] Andriotis A N, Menon M, Srivastava D and Chernozatonskii L 2001 *Phys. Rev. Lett.* **87** 066802
[67] Kim D-H, Sim H-S and Chang K J 2001 *Phys. Rev.* B **64** 115409
[68] Hjort M and Stafström S 2001 *Phys. Rev.* B **63** 113406
[69] Mingo N, Han J, Anantram M P and Yang L 2001 *Surf. Sci.* **482** 1130
[70] Andriotis A N and Menon M 2001 *J. Chem. Phys.* **115** 2737
[71] Taylor J, Guo H and Wang J 2001 *Phys. Rev.* B **63** 245407
[72] Mingo N, Yang L and Han J 2001 *J. Phys. Chem.* **105** 11 142
[73] Caroli C, Combescot R, Nozieres P and Saint-James D 1971 *J. Phys. C: Solid State Phys.* **4** 916
[74] Caroli C, Combescot R, Lederer D, Nozieres P and Saint-James D 1971 *J. Phys. C: Solid State Phys.* **4** 2598
[75] Combescot R 1971 *J. Phys. C: Solid State Phys.* **4** 2611
[76] Caroli C, Combescot R, Nozieres P and Saint-James D 1972 *J. Phys. C: Solid State Phys.* **5** 21
[77] Tsymbal E Y and Pettifor D G 1996 *J. Phys.: Condens. Matter* **8** L569
[78] Todorov T N, Tsymbal E Y and Pettifor D G 1996 *Phys. Rev.* B **54** 12 685
[79] Tsymbal E Y and Pettifor D G 1996 *Phys. Rev.* B **54** 15 314
[80] Mathon J 1997 *Phys. Rev.* B **55** 960
[81] Tsymbal E Y and Pettifor D G 1997 *J. Phys.: Condens. Matter* **9** L411
[82] Tsymbal E Y and Pettifor D G 1998 *Phys. Rev.* B **58** 432
[83] Tsymbal E Y and Pettifor D G 1999 *J. Appl. Phys.* **85** 5801
[84] Sanvito S, Lambert C J, Jefferson J H and Bratkovsky A M 1999 *Phys. Rev.* B **59** 11 936
[85] Tsymbal E Y and Pettifor D G 2000 *Phys. Rev.* B **61** 506
[86] Bozec D, Howson M A, Hickey B J, Shatz S, Wiser N, Tsymbal E Y and Pettifor D G 2000 *Phys. Rev. Lett.* **85** 1314
[87] Tsymbal E Y 2000 *Phys. Rev.* B **62** 3608
[88] Tsymbal E Y and Pettifor D G 2001 *Solid State Phys.* **56** 113
[89] Todorov T N and Sutton A P 1993 *Phys. Rev. Lett.* **70** 2138
[90] Bratkovsky A M, Sutton A P and Todorov T N 1995 *Phys. Rev.* B **52** 5036
[91] Todorov T N and Sutton A P 1996 *Phys. Rev.* B **54** 14 234

[92] Sirvent C, Rodrigo J G, Vieira S, Jurczyszyn L, Mingo N and Flores F 1996 *Phys. Rev.* B **53** 16 086
[93] Levy Yeyati A, Martin-Rodero A and Flores F 1997 *Phys. Rev.* B **56** 10 369
[94] Cuevas J C, Levy Yeyati A and Martin-Rodero A 1998 *Phys. Rev. Lett.* **80** 1066
[95] Cuevas J C, Levy Yeyati A, Martin-Rodero A, Rubio Bollinger G, Untiedt U and Agrait N 1998 *Phys. Rev. Lett.* **81** 2990
[96] Scheer E, Agrait N, Cuevas J C, Levy Yeyati A, Ludolph B, Martin-Rodero A, Rubio Bollinger G, van Ruitenbeek J M and Urbina C 1998 *Nature* **394** 154
[97] Brandbyge M, Kobayashi N and Tsukada M 1999 *Phys. Rev.* B **60** 17 064
[98] Hansen K, Nielsen S K, Brandbyge M, Laegsgaard E, Stensgaard I and Besenbacher F 2000 *Appl. Phys. Lett.* **77** 708
[99] Todorov T N, Hoekstra J and Sutton A P 2000 *Phil. Mag.* B **80** 421
[100] Sutton A P, Todorov T N, Cawkwell M J and Hoekstra J 2001 *Phil. Mag.* A **81** 1833
[101] Hoekstra J, Sutton A P, Todorov T N and Horsfield A P 2000 *Phys. Rev.* B **62** 8568
[102] Todorov T N, Hoekstra J and Sutton A P 2001 *Phys. Rev. Lett.* **86** 3606
[103] Todorov T N 2001 *J. Phys.: Condens. Matter* **13** 10 125
[104] Todorov T N 1999 *Phil. Mag.* B **79** 1577
[105] Ness H and Fisher A J 1999 *Phys. Rev. Lett.* **83** 452
[106] Ness H, Shevlin S A and Fisher A J 2001 *Phys. Rev.* B **63** 125422
[107] Payne M C 1989 *J. Phys.: Condens. Matter* **1** 4931
[108] Landauer R 1989 *J. Phys.: Condens. Matter* **1** 8099
[109] McLennan M J, Lee Y and Datta S 1991 *Phys. Rev.* B **43** 13 846
[110] Torres J A, Pascual J I and Saenz J J 1996 *Phys. Rev.* B **49** 16 581
[111] Lang N D 1995 *Phys. Rev.* B **52** 5335
[112] Emberly E and Kirczenov 1998 *Phys. Rev. Lett.* **81** 5205
[113] Gutierrez R, Grossmann F, Knospe O and Schmidt R 2001 *Phys. Rev.* A **64** 013202
[114] Cohen M H, Falicov L M and Phillips J C 1962 *Phys. Rev. Lett.* **8** 316
[115] Jauho A-P, Wingreen N S and Meir Y 1994 *Phys. Rev.* B **50** 5528
[116] Lee P A and Fisher D S 1981 *Phys. Rev. Lett.* **47** 882
[117] Büttiker M, Imry Y, Landauer R and Pinhas S 1985 *Phys. Rev.* B **31** 6207
[118] Di Ventra M, Pantelides S T and Lang N D 2000 *Phys. Rev. Lett.* **84** 979
[119] Sutton A P, Finnis M W, Pettifor D G and Ohta Y 1988 *J. Phys. C: Solid State Phys.* **21** 35
[120] Paulsson M and Stafström S 2001 *Phys. Rev.* B **64** 035416
[121] Pernas P L, Martin-Rodero A and Flores F 1990 *Phys. Rev.* B **41** 8553
[122] Landauer R 1987 *Z. Phys.* B **68** 217
[123] Landauer R 1992 *Phys. Scr.* T **42** 110
[124] Landauer R 1957 *IBM J. Res. Dev.* **1** 223
[125] Landauer R 1988 *IBM J. Res. Dev.* **32** 306
[126] Payne M C and Engel G E 1990 *J. Phys.: Condens. Matter* **2** 1355
[127] Sorbello R S 1981 *Phys. Rev.* B **23** 5119
[128] Lenk R 1990 *Phys. Status Solidi* b **161** 797
[129] Zwerger W, Bönig L and Schönhammer K 1991 *Phys. Rev.* B **43** 6434
[130] Kunze C 1994 *J. Phys.: Condens. Matter* **6** 10 011
[131] Kunze C 1995 *Phys. Rev.* B **51** 6979
[132] Reuss M and Zwerger W 1996 *Phys. Rev.* B **53** 9513
[133] Zwerger W 1997 *Phys. Rev. Lett.* **79** 5270
[134] Sorbello R S 1998 *Superlatt. Microstruct.* **23** 711
[135] Sutton A P and Todorov T N 1998 *Boundaries and Interfaces in Materials: the David A. Smith Symp.* ed R C Pond, W A T Clark, A H King and D B Williams (Warrendale, PA: The Minerals, Metals and Materials Society) p 189
[136] Calvayrac F, Reinhard P-G, Suraud E and Ullrich C A 2000 *Phys. Rep.* **337** 493
[137] Theilhaber J 1992 *Phys. Rev.* B **46** 12 990
[138] Finnis M W, Paxton A T, Methfessel M and van Schilfgaarde M 1998 *Phys. Rev. Lett.* **81** 5149
[139] Elstner M, Porezag D, Jungnickel G, Elsner J, Haugk M, Frauenheim Th, Suhai S and Seifert G 1998 *Phys. Rev.* B **58** 7260
[140] Kunert T and Schmidt R *Phys. Rev.* A 2002 submitted
[141] Di Ventra M and Pantelides S T 2000 *Phys. Rev.* B **61** 16 207
[142] Todorov T N 1998 *Phil. Mag.* B **77** 965
[143] Gurevich V L 1997 *Phys. Rev.* B **55** 4522